

行政院國家科學委員會專題研究計畫 成果報告

經 Photo-fries 重排的新高分子型光安定劑之研究

計畫類別：個別型計畫

計畫編號：NSC91-2216-E-009-015-

執行期間：91年08月01日至92年07月31日

執行單位：國立交通大學應用化學研究所

計畫主持人：林木獅

計畫參與人員：林木獅、李承智、趙浚佑、莊絢仁、林志浩

報告類型：精簡報告

處理方式：本計畫可公開查詢

中 華 民 國 92 年 10 月 29 日

經由 Photo-Fries'重排反應的新高分子型光安定劑之研究

摘 要

高分子材料經常在戶外長期使用，因此材料的耐候性就變得很重要，維持高分子的光安定化有許多方法，例如：加入 UV 遮蔽劑、激發態的去活化劑、自由基的消除劑及 UV 吸收劑。UV 吸收劑會將所吸收的 UV 光能消耗並轉成不會傷害材料的熱能，降低輻射能的不利影響，故較常被使用。一些已商業化的光吸收劑，大半都是低分子量的鄰羥基苯酮或其衍生物，當高分子材料使用這些低分子量的 UV 吸收劑時，常會出現的缺點，例如長期在戶外使用時會滲出表面或加工時受熱揮發，如果提高添加量，卻又會造成材料機械物性下降。為了改進這些缺失，本篇研究加入新穎性高分子型的光安定劑，第一章首先研究 PPA 及 PMPA，結果顯示，PPA 及 PMPA 會進行 Photo-Fries 重排反應，在分子主結構上產生具光安定效果的鄰羥基苯酮，兩者的反應速率常數不同，並且以 PMPA 的光安定效果較佳。在第二章則將 PPA 及 PMPA 加入 PET 中，觀察它們對 PET 的光安定效果及保護作用，並證實有效。這個觀念亦可推廣應用到於熱固性聚合物，因此在第三章中以環氧乙烷及二丙烯酸雙苯酚 A 酯形成 IPN 聚合物，經 UV 照光後亦同樣產生鄰羥基苯酮，因此可達到 IPN 聚合物的光安定化效果。

本研究結論，確實可達到以 Photo-Fries 重排反應產生新穎性聚合物級的光安定劑，並具有良好的安定化效果。

ABSTRACT

Long term out-door uses of polymers are very common. Therefore, the weatherability of polymers becomes an important consideration. Photostabilization of polymers can be achieved by different means. These include screen of ultraviolet light, deactivation of excited states, addition of radical scavengers, and uv absorbers. Use of uv absorbers to dissipate the photo energy and convert it into a harmless heat, and therefore, to retard the adverse effect of irradiation is widely applied in polymer technology. However, most commercial uv absorbers are low molecular weight derivatives of o-hydroxybenzophenone. When these low molecular weight uv absorbers are incorporated into polymers, many drawbacks occur quite often, such as leaching problem during long term out-door application and evaporation problem during thermal processing. Furthermore, when these uv absorbers are

incorporated into polymer in large quantities, drawback of mechanical properties are often observed. In order to avoid these drawbacks, we are interested in innovative high molecular weight polymeric types of photostabilizers. In a kinetic and mechanism study of photo-fries' rearrangement for poly(phenyl acrylate) (PPA) and poly(p-methylphenyl acrylate) (PMPA), both acrylic polymers underwent photo-fries' rearrangement, leading to the production of o-hydroxybenzophenone moiety at the pendant group in different rate constants, and both were expected to be inherent photostabilizers, with PMPA a better one (chapter 1). Both PPA and PMPA were then used to protect thermoplastics against photodegradation and their protection to PET was confirmed (chapter 2). The same idea also applied to thermosetting polymers. Thus, an interpenetrating polymer networks (IPN) based on epoxy and bisphenol-A diacrylate was proved to produce o-hydroxybenzophenone moiety when this material was under uv irradiated. And its photostabilization of IPN materials was successfully achieved (chapter 3). In conclusions, innovative polymeric types of photostabilizers via photo-fries' rearrangement has been successfully developed in this research.

Chapter 1. Kinetics and Mechanism of Intramolecular Photo-Fries' Rearrangement by Model Polymers: PPA and PMPA

1.1 ABSTRACT

Poly(phenyl acrylate) (PPA) and poly(p-methylphenyl acrylate) (PMPA) were synthesized and characterized. Upon irradiation of ultraviolet light ranging from 275 to 360 nm, both PPA and PMPA underwent intra-molecular Photo-Fries rearrangement, leading to the formation of both o- and p-hydroxybenzophenones from PPA, and only o-hydroxybenzophenone from PMPA. The intra-molecular hydrogen-bonded six-membered ring structure of o-hydroxybenzophenone moiety is well known as a UV-stabilizer. A kinetic study of this photo-Fries rearrangement was investigated by using FTIR to monitor the functional group changes. Experimental result revealed a continuous α -cleavage of the ester group at $\nu_{C=O}$ 1750 cm^{-1} and ν_{C-O-C} 1195-1202 cm^{-1} . The kinetic data fitted a first-order of reaction, with a rate constant of $3.91 \times 10^{-1} \text{ day}^{-1}$ for PMPA and $3.10 \times 10^{-2} \text{ day}^{-1}$ for PPA. Furthermore, conversion of PMPA was found to reach an earlier leveling off than PPA. Resonance stabilization of a tertiary radical intermediate adjacent to the p-methyl group in PMPA accounts for the experimental result and supports a dissociative radical mechanism for solid photo-fries' rearrangement, similar to the solution cage mechanism reported in literature.

1.2 INTRODUCTION

O-hydroxybenzophenone and its derivatives are believed to be effective photostabilizers against photodegradation and photo-oxidation [1,2,3]. Poly(phenyl acrylate)(PPA) is able to undergo Photo-Fries rearrangement upon irradiation of ultraviolet light [4-9]. In search of literature, two mechanisms were proposed to interpret the production of o- and p-hydroxybenzophenones. In bondage mechanism, the acyl portion and phenoxy portion are bonded to the

benzene ring all the way through the whole process [5,6,7]. While in the solvent cage mechanism [7,8,9], the homolytical α -cleavage at the ester group leads to separated acyl and phenoxy radicals, which are included in solvent cage, followed by rearrangement and recombination to form o- and p-acylcyclohexadieneones and, finally to o- and p-hydroxybenzophenones via tautomerism. However, there is lack of evidence to identify which mechanism is right. Of the two products, only o-hydroxybenzophenone is able to form an intra-molecular hydrogen-bonded six membered ring structure which acts as a UV-absorber [1]. In order to study the reactivity of Photo-Fries reaction, kinetic studies of PPA and PMPA were carried out by irradiation with ultraviolet light. A comparison of rate constants between PPA and PMPA would be able to interpret the mechanism and suggest a better polymer type of inherent photo-stabilizer. In this article we report such a study.

1.3 EXPERIMENTAL

1.3.1 Syntheses of Phenyl acrylate and p-Methylphenyl acrylate

Into a 300-mL four-necked flask, equipped with a mechanical stirrer, a thermometer and a dry tube, phenol (0.5 mole) and triethylamine (0.5 mole) were charged. Acryloyl chloride (0.5 mole) was then added dropwise, keeping the temperature below 10 °C. Esterification proceeded for 10 hours. Then the reaction mixture was washed twice with distilled water to remove the triethylamine salt, followed by washing with 6 % NaOH solution to remove the unreacted phenol and, finally by washing with distilled water again until the solution became neutral. The oily product was dried with MgSO₄ and distilled under reduced pressure (72 °C/3 torr) to yield 85 % of phenyl acrylate. P-methylphenyl acrylate was prepared exactly by the same way, except using p-cresol to replace phenol. The pale yellow oily p-methylphenyl acrylate thus obtained (under 83.5 °C/3 torr) was 69 % of yield.

1.3.2 Syntheses of PPA and PMPA

Into a three-necked flask, equipped with a condenser and a thermometer, was charged one volume of phenyl acrylate in ten volumes of benzene. Recrystallized benzoyl peroxide (0.5 % on phenyl acrylate) was added as initiator. The mixture was heated to reflux for 22 hours, then was coagulated in petroleum ether. A pale yellow PPA was filtered and dried in a vacuum oven at 60 °C for 10 hours. PMPA was prepared exactly by the same way.

1.3.3 Instruments

Chemical structure identifications were done with a Bruker AM-300 ¹HNMR and a Nicolet 520 FTIR with a resolution of 1 cm⁻¹. Glass transition temperatures were obtained with Seiko SSC 5200 DSC. Solution viscosity was measured with a Ubbelohde capillary viscometer at 25 °C. Molecular weights and molecular weight distribution (MWD) were characterized with GPC, calibrating with standard polystyrene.

1.3.4 Photo-Fries Rearrangement

Commercial UV lamps (UVB-313), emitting UV range 275 to 360 nm with a maximum intensity at 313 nm were selected for our study. PPA (or PMPA) films was cast on Al plate and dried, and were irradiated in a QUV accelerated weathering tester [10] with eight UVB-313 fluorescent UV lamps (with 40 watts of each lamp). The functional group changes at various time were monitored with FTIR by placing the sample in a reflecting type sample cell (Buck Scientific). The conversion, α , is defined by

$$\alpha = (C_t - C_0)/(C_\infty - C_0) = (A_t - A_0)/(A_\infty - A_0) \quad (1)$$

Where A_0 , A_t , A_∞ are the absorbances of ν_{C-O-C} before irradiation, at irradiation time t , and at infinitive time (level off). C_0 , C_t and C_∞ are the corresponding concentrations of the specific group. The difference spectra $A_t - A_0$ were

obtained by subtracting absorbances at t from that before irradiation, using benzene absorption at 1595 cm^{-1} as internal standard [11].

1.4 RESULTS and DISCUSSION

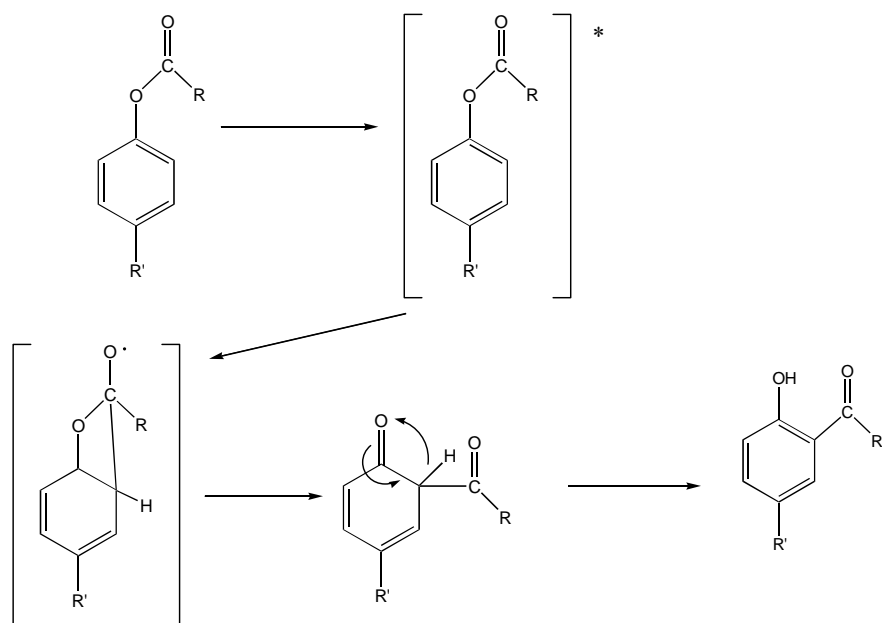
The synthesized phenyl acrylate shows its ^1H NMR spectrum in [Figure 1-1](#). Integration of peaks at δ 7.10 to 7.39 ppm (multiplet) shows five protons on the phenyl ring. The peaks at δ 6.55 ppm (doublet) indicates one proton on the vinyl group (trans), that at δ 5.94 ppm (doublet) is another proton on vinyl (cis). While the other cis proton on vinyl group occurs at δ 6.30 ppm (quartet). [Figure 1-2](#) shows its FTIR spectrum. The carbonyl absorption of the ester group occurs at 1750 cm^{-1} , that of C-O-C stretching occurs at 1195 cm^{-1} . While the absorption of C=C occurs at 1631 cm^{-1} . [Figure 1-3](#) shows the FTIR spectrum of PPA. Absorptions of $\nu_{\text{C=O}}$ and $\nu_{\text{C-O-C}}$ occur at 1750 and 1195 cm^{-1} , respectively. Missing absorption at 1631 cm^{-1} indicates the disappearance of C=C by forming PPA. [Figure 1-4](#) shows the ^1H NMR spectrum of p-methylphenyl acrylate. Integration of peaks at δ 6.98 to 7.19 ppm (multiplet) indicates four protons on the phenyl ring. The trans H occurs at δ 6.56 ppm (doublet). The other two cis H's occur at 5.97 ppm (doublet) and 6.30 ppm (quartet). The three protons on the methyl group occurs at δ 2.30 ppm (singlet). Its FTIR spectrum ([Figure 1-5](#)) reveals a carbonyl stretching of the ester at 1748 cm^{-1} , that of C-O-C at 1202 cm^{-1} , and that of C=C stretching at 1636 cm^{-1} . PMPA shows its FTIR spectrum in [Figure 1-6](#). The $\nu_{\text{C=O}}$ and $\nu_{\text{C-O-C}}$ absorptions occur at 1745 and 1202 cm^{-1} . Again, the missing absorption at 1636 cm^{-1} indicates the disappearance of C=C by forming PMPA. The PPA and PMPA have inherent viscosities of 0.13 and 0.17, respectively. The PPA has an average molecular weight of 9600 with a molecular weight distribution of 1.50 obtained with GPC. While PMPA has an average molecular weight of 9700 with a molecular weight distribution of 1.46. Both PPA and PMPA have sharp glass transition temperatures at 59.5 and $64.6\text{ }^\circ\text{C}$, respectively ([Figure 1-7](#)).

During irradiation of ultraviolet ranging 275 to 360 nm, the intra-molecular photo-fries rearrangement were evidenced from the continuous decreasing absorbances of $\nu_{C=O}$ and ν_{C-O-C} for both PPA and PMPA. Typical difference spectra of $A_t - A_0$ (t in days) are given in [Figure 1-8](#). It is noted that a newly increasing absorption of $\nu_{C=O}$ for the products of o- and/or p-hydroxybenzophenones at 1725 interferes with the decreasing absorption of $\nu_{C=O}$ at 1745-1750 cm^{-1} for ester group. Fortunately, in view of the Norrish I reaction where the α -cleavage at C-O-C indicates a smooth decreasing of absorption, without interference of other groups. We, therefore, chose the data of C-O-C disappearance for our kinetic analyses. Integration of $A_t - A_0$ divided by the area of $A_\infty - A_0$ gives the conversion, α , according to equation (1). Plots of the conversion of C-O-C disappearance, α , versus time for PPA and PMPA are given in [Figures 1-9 and 1-10](#). The kinetic data fit a first-order of reaction according to

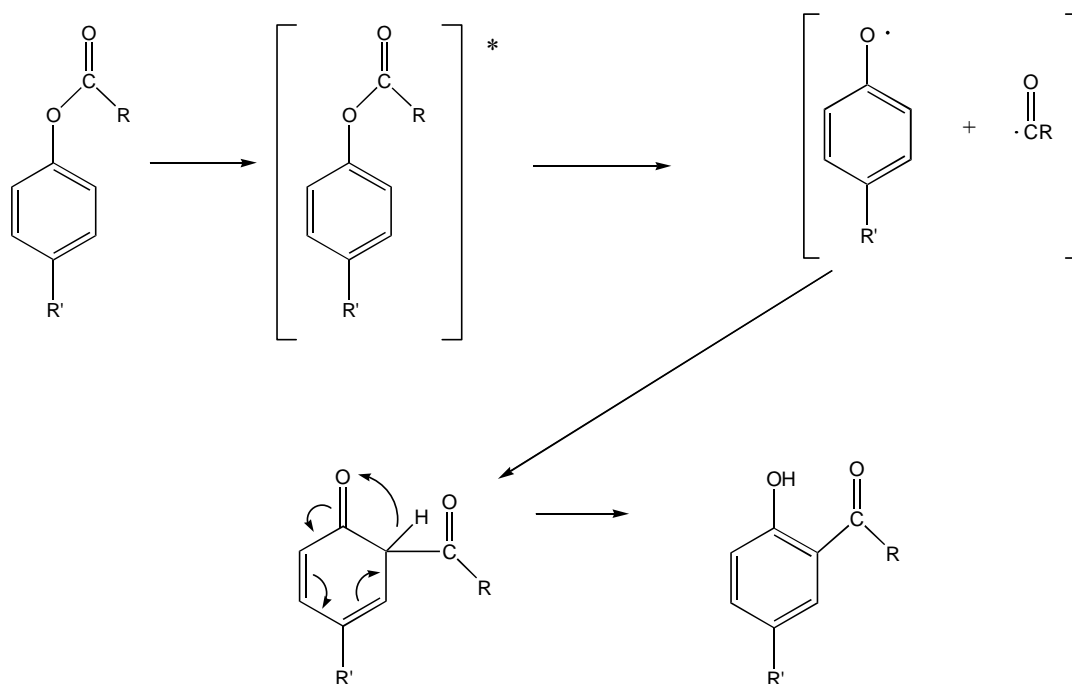
$$- \ln (1 - \alpha) = k t$$

Where k and t represent the rate constant and irradiation time. It is noted that the conversion of PMPA reached an earlier leveling off than PPA, meaning a faster reaction of PMPA than PPA. Plots of $-\ln (1 - \alpha)$ versus t for PPA and PMPA are given in [Figure 1-11](#). The rate constants for the photo-fries reaction can be found from slopes, which are $3.10 \times 10^{-2} \text{ day}^{-1}$ for PPA and $3.91 \times 10^{-1} \text{ day}^{-1}$ for PMPA, respectively.

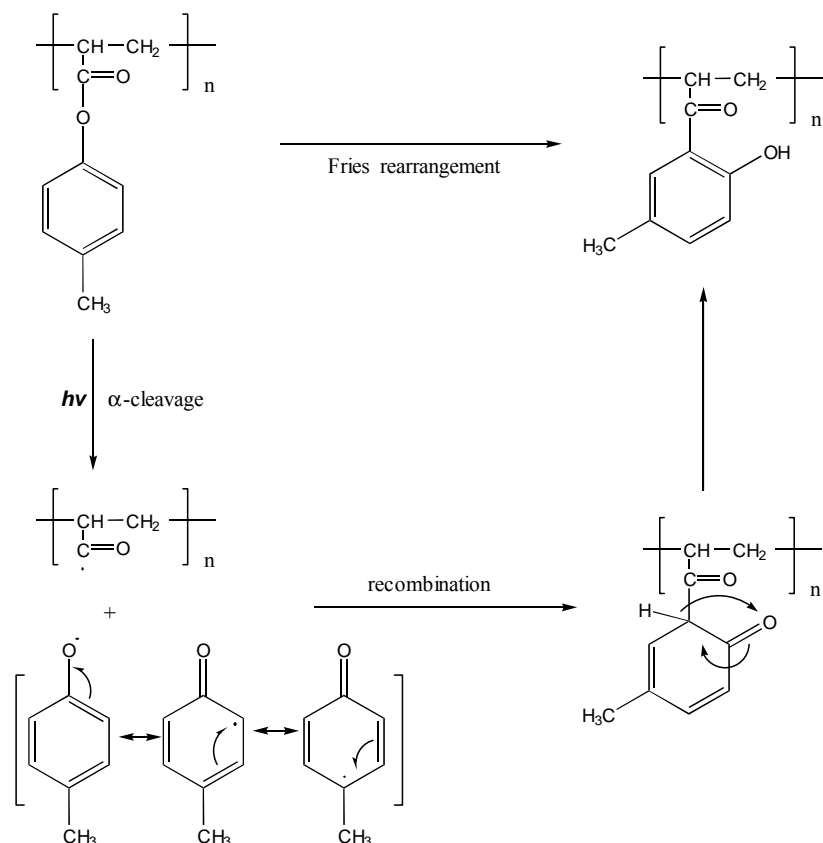
Two mechanisms are proposed for the photo-fries rearrangement in literature [4-9]. Sanders, Hedaya and Trecker proposed a bondage mechanism, in which the acyl and phenoxy portions of the molecule remaining bonded to each other throughout the entire course of the rearrangement [7].



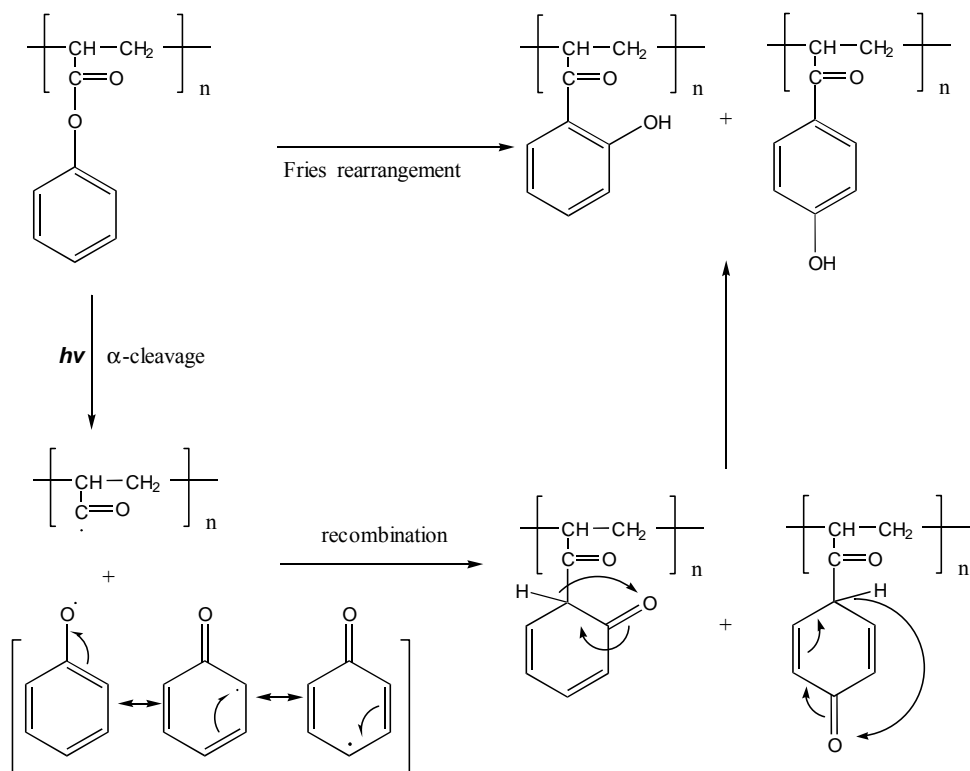
The other, known as the solution cage mechanism, was proposed by Kobsa [8]. This mechanism involves a homolytical α -cleavage at the C-O-C bond of ester, giving rise to acyl and phenoxy radicals which are held within a solution cage, followed by recombination of radicals to form o-acylcyclohexadieneone and p-acylcyclohexadieneone and, finally to o- and p-hydroxybenzophenones by tautomerism.



Li and Guillet, in their study of photo-fries reaction in solid PPA, reported that the formation of both o- and p-hydroxybenzophenone groups in solid PPA required similar activation energies as for solution cage processes in simple radical recombination [6]. In comparison of rate constants for PPA and PMPA in our present study, it appears that the higher rate constant for PMPA support Li and Guillet's result. During photo-fries reaction, the separated phenoxy radical in the intermediate is stabilized by resonance form of a quinone type structure with the odd electron on the para carbon connecting to the methyl group, forming a stable tertiary free radical in the resonance forms:



Such an intermediate involving a tertiary radical would be more stable than that involving all secondary radicals in the resonance forms from PPA:



Therefore, in view of the higher rate constant of PMPA, almost an order higher than that of PPA during photo-fries rearrangement, it can be reasonably inferred that due to the resonance stabilization of the intermediate in the form of a stable tertiary radical, the intra-molecular photo-fries rearrangement follows a dissociative radical pathway, similar to the solution cage mechanism as proposed by Kobsa [8].

During photo-fries' reaction, PPA produced at a lower rate both o- and p-hydroxybenzophenones. As is well known in literature, only the ortho derivative is an effective uv-absorber [1,2,3]. Since PMPA produced only the effective ortho derivative at a faster rate, therefore PMPA is believed to be a more effective photostabilizer than PPA. Paper on this confirmation of photostabilization based on fibers of PPA/PET and PMPA/PET blends are submitted to Polym. Degrad. & Stab. [12]

1.5 CONCLUSIONS

In a comparison of the photo-fries rate constants for PPA and PMPA, the higher rate constant of PMPA supported a dissociative radical mechanism similar to the solution cage mechanism as proposed by Kobsa. PMPA produced the effective uv-absorber, o-hydroxybenzophenone, at a higher rate than PPA and consequently PMPA is expected to be a more effective photostabilizer.

1.6 REFERENCES

1. W. Schnabel, "Polymer Degradation", Hanser International, distributed in USA by Macmillan Publishing, 1981, Ch. 4, pp.117-120.
2. W. L. Hawkins (ed.), "Polymer Stabilization", John Wiley & Sons, New York, 1972, p. 197.
3. M. S. Lin, M. W. Wang and L. A. Chang, "Photostabilization of Epoxy by Forming IPNs with Bisphenol-A Diacrylate", Polym. Degrad. & Stab., 66,

343 (1999).

4. J. C. Anderson, and C. B. Reese, *J. Chem. Soc.*, 1781 (1961).
5. J. C. Anderson, and C. B. Reese, *Proc. Chem. Soc.*, 217 (1960).
6. S. K. L. Li, and J. E. Guillet, *Macromolecules*, 10(4), 840 (1977).
7. M. R. Sandner, E. Hefaya, and D. J. Trecker, *JACS.*, 90, 7249 (1968).
8. H. Kobsa, *J. Org. Chem.*, 27, 2293 (1962).
9. R. A. Finnegan, and J. J. Mattice, *Tetrahedron*, 21, 1015 (1965).
10. QUV accelerated weathering tester, Q-Panel Co., with UVB 313 fluorescent UV lamps, 40 watts x 8.
11. L. Konig, *Appl. Spectr.*, 29, 293 (1975).
12. M. S. Lin, C. T. Lee, and C. F. Wu, paper submitted to *Polym. Degrad. & Stab.*, 2003.

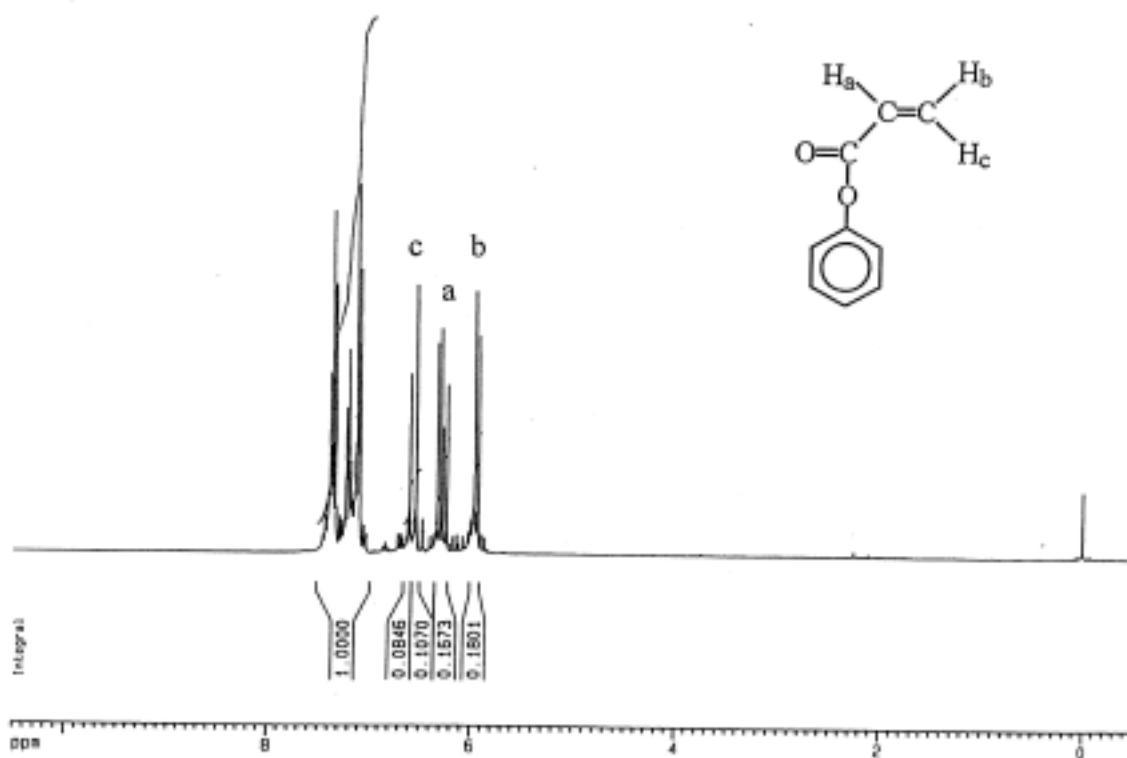


Figure 1-1 ¹H NMR spectrum of phenyl acrylate.

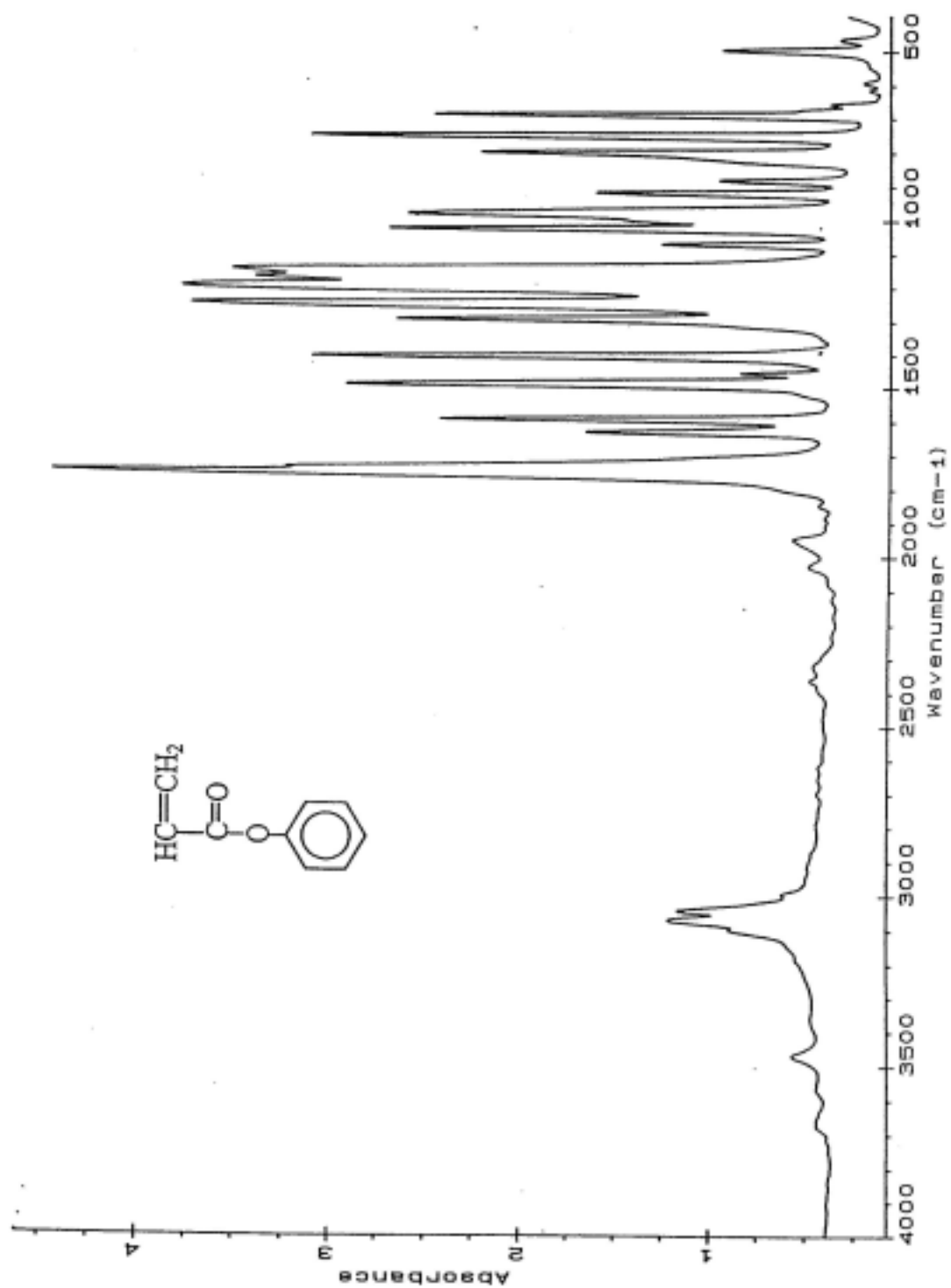


Figure 1-2 FTIR spectrum of phenyl acrylate.

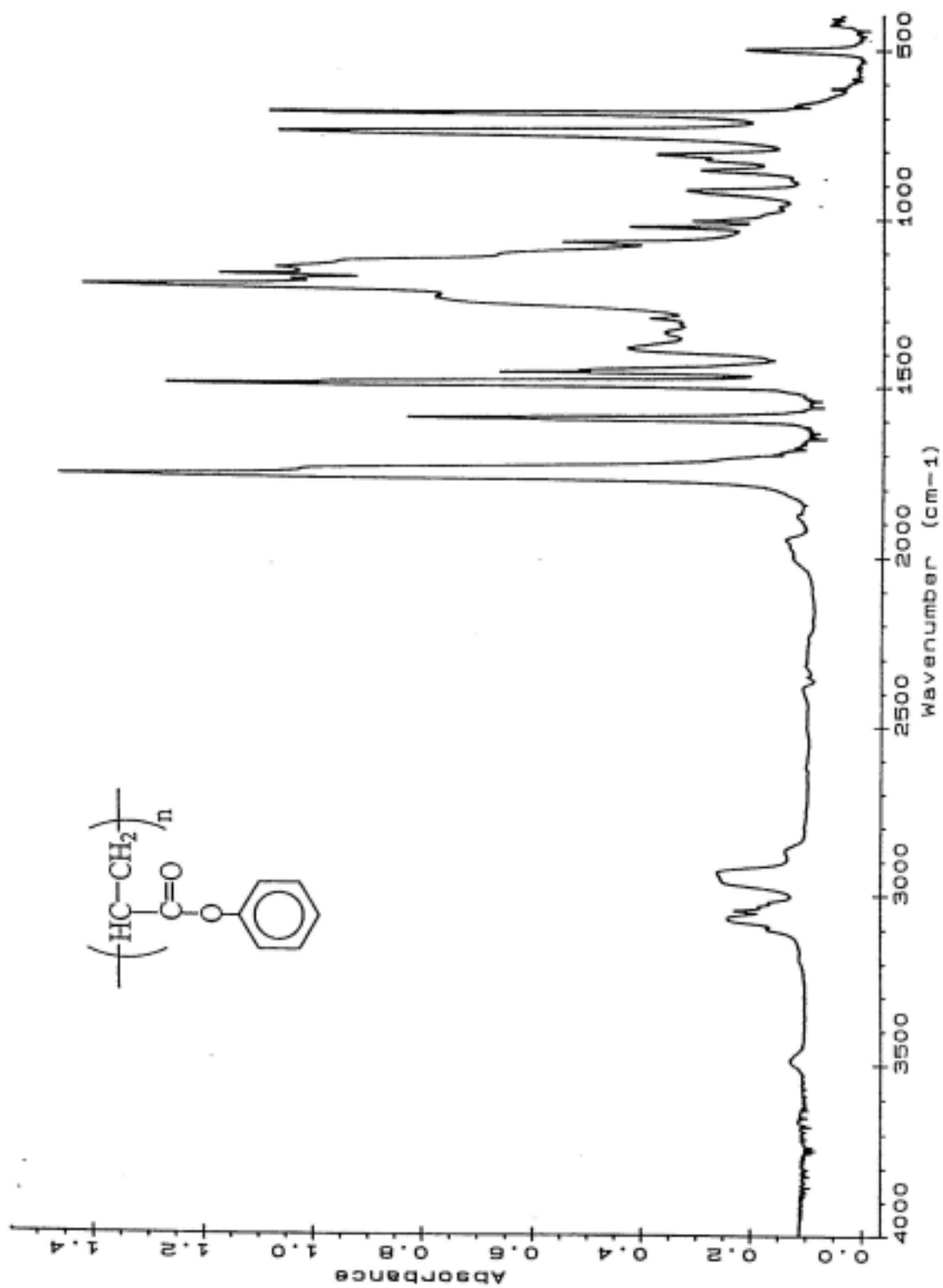


Figure 1-3 FTIR spectrum of poly(phenyl acrylate).

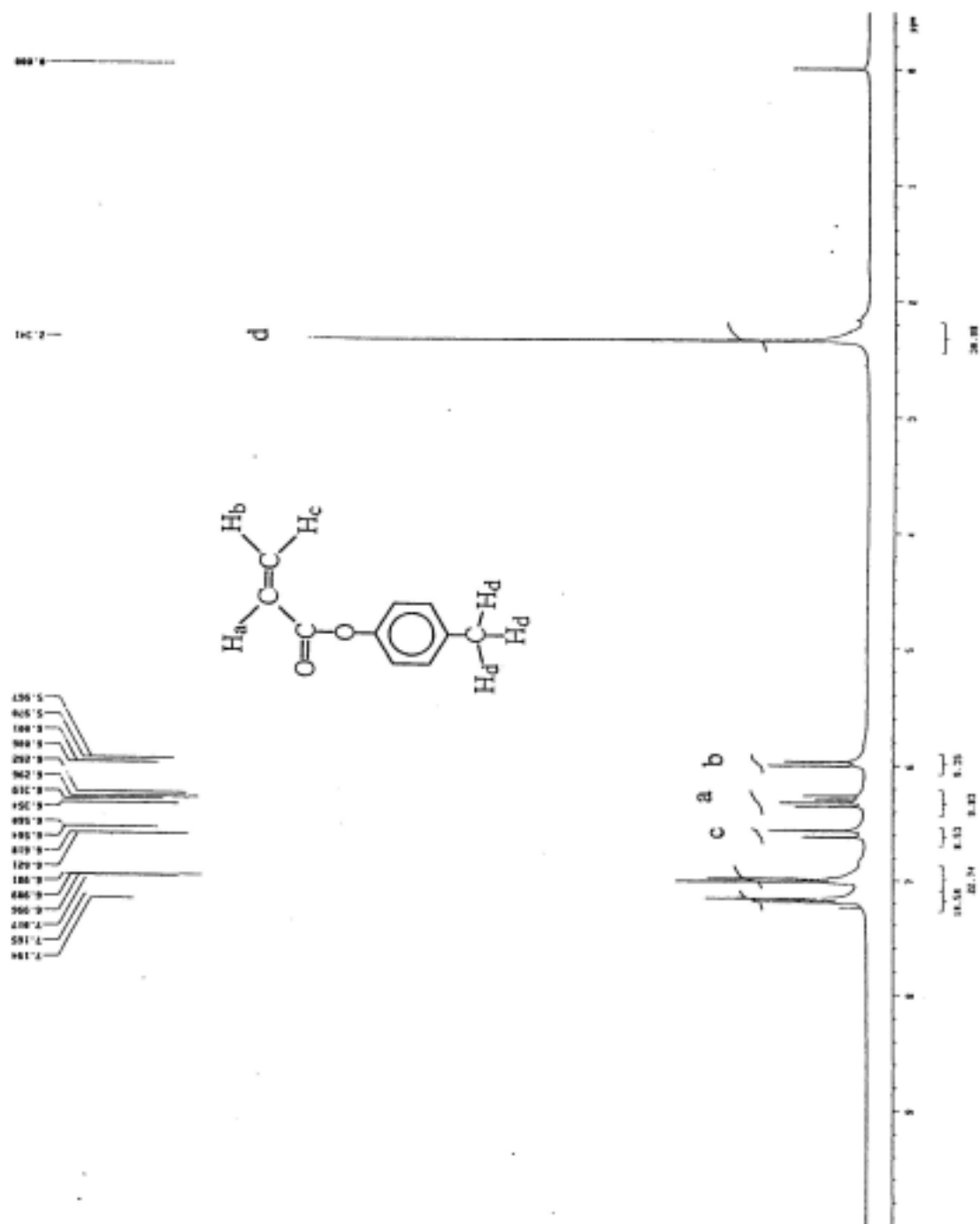


Figure 1-4 1H NMR spectrum of p-methylphenyl acrylate.

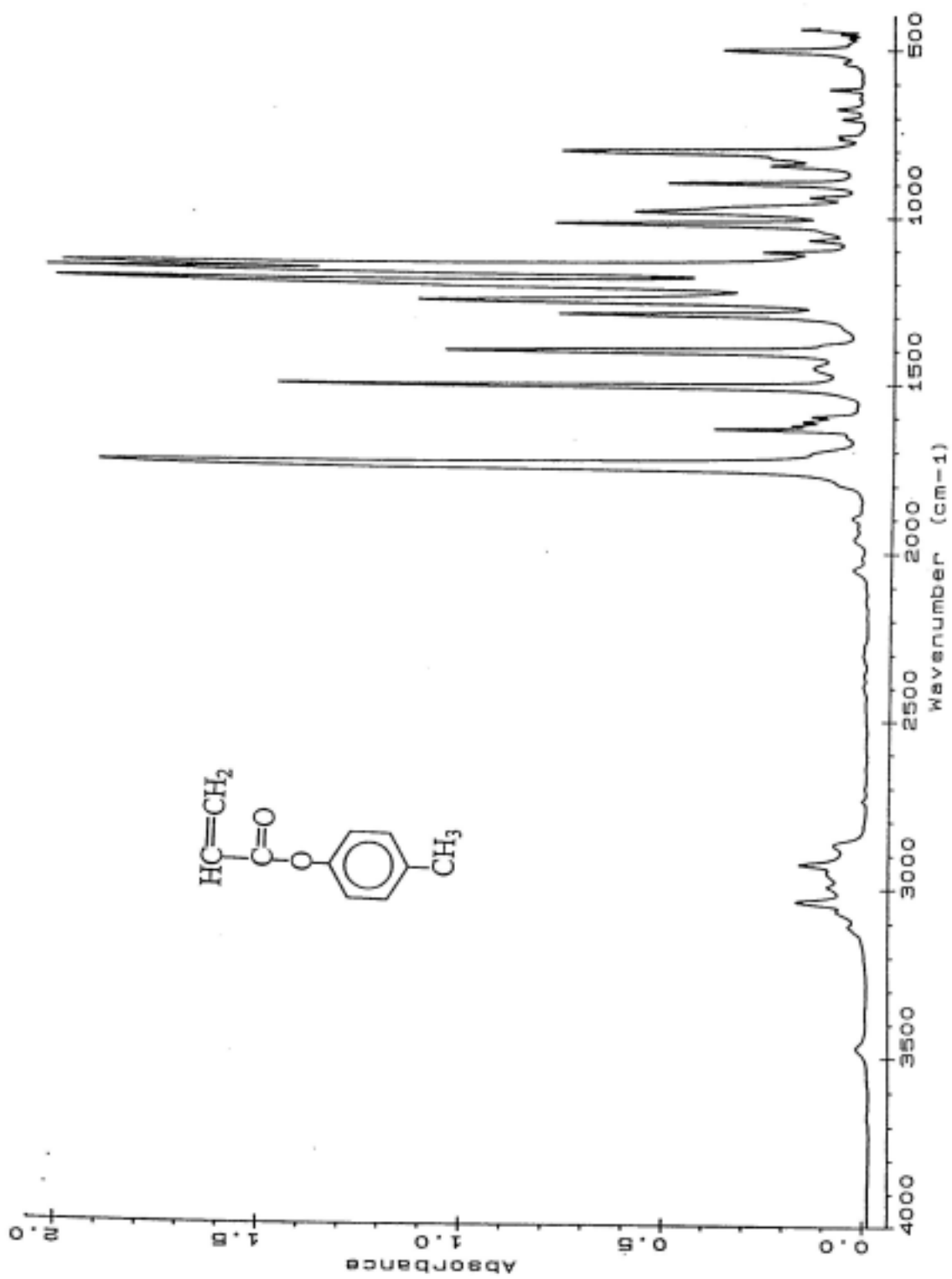


Figure 1-5 FTIR spectrum of p-methylphenyl acrylate.

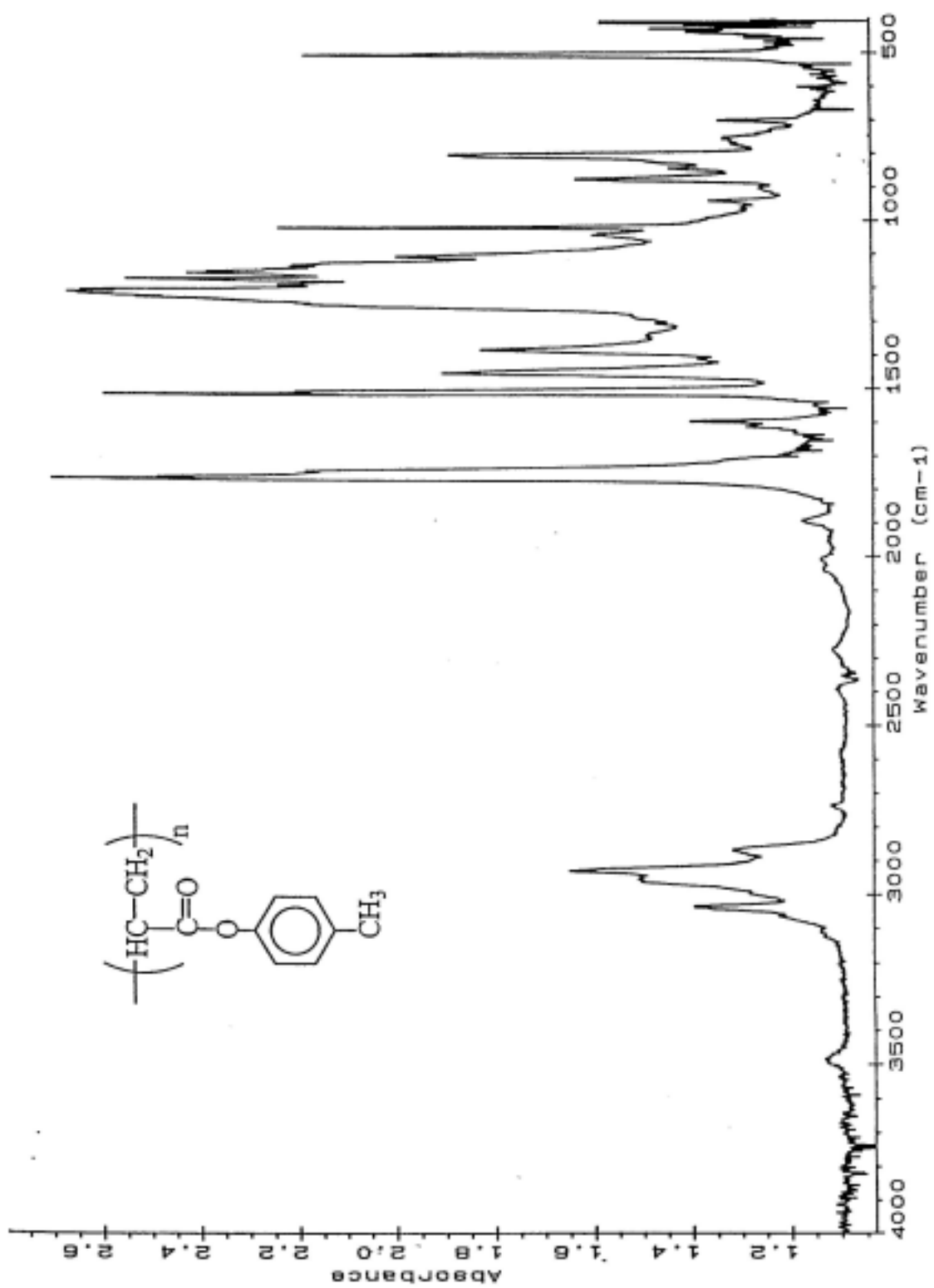


Figure 1-6 FTIR spectrum of poly(p-methylphenyl acrylate).

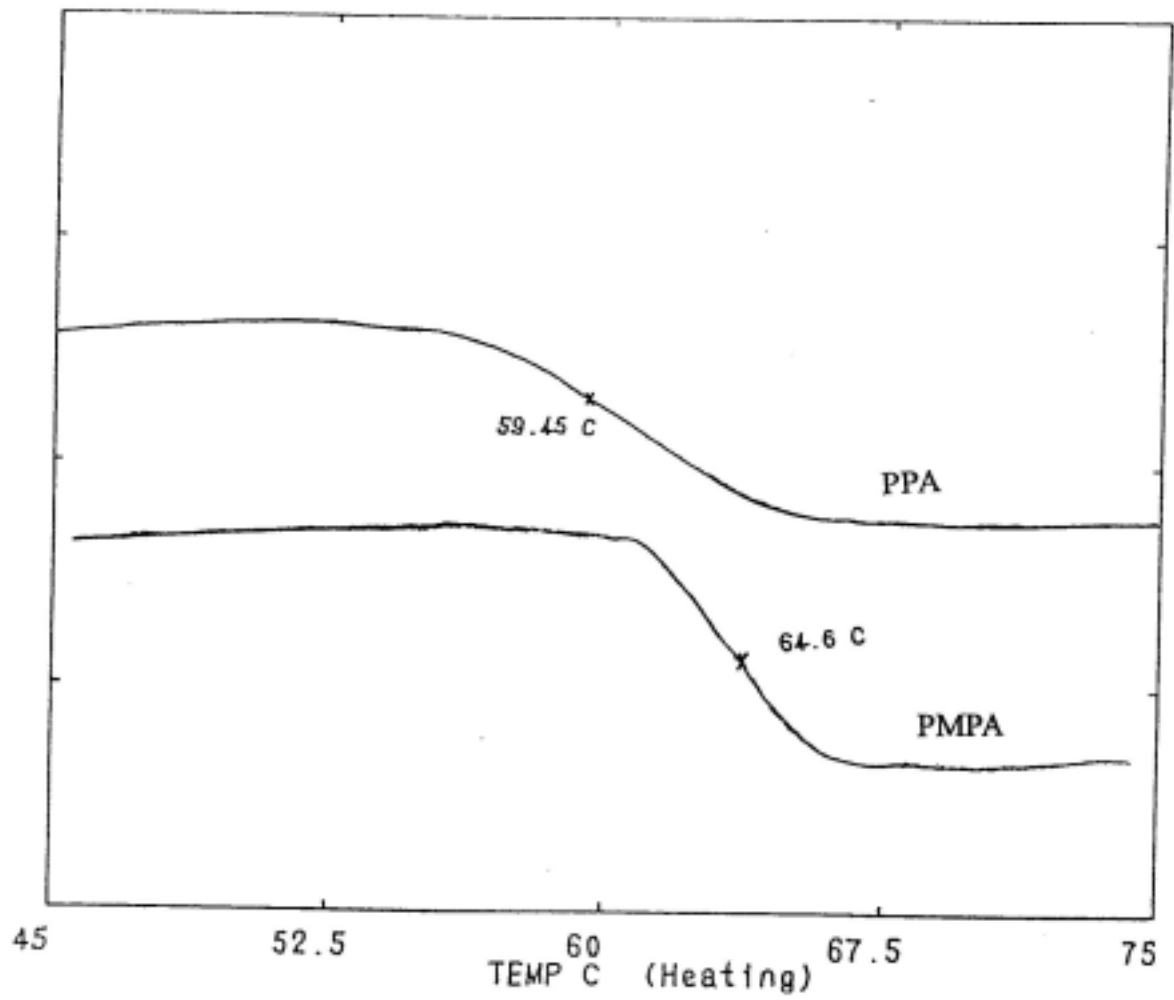


Figure 1-7 DSC thermograms for PPA and PMPA.

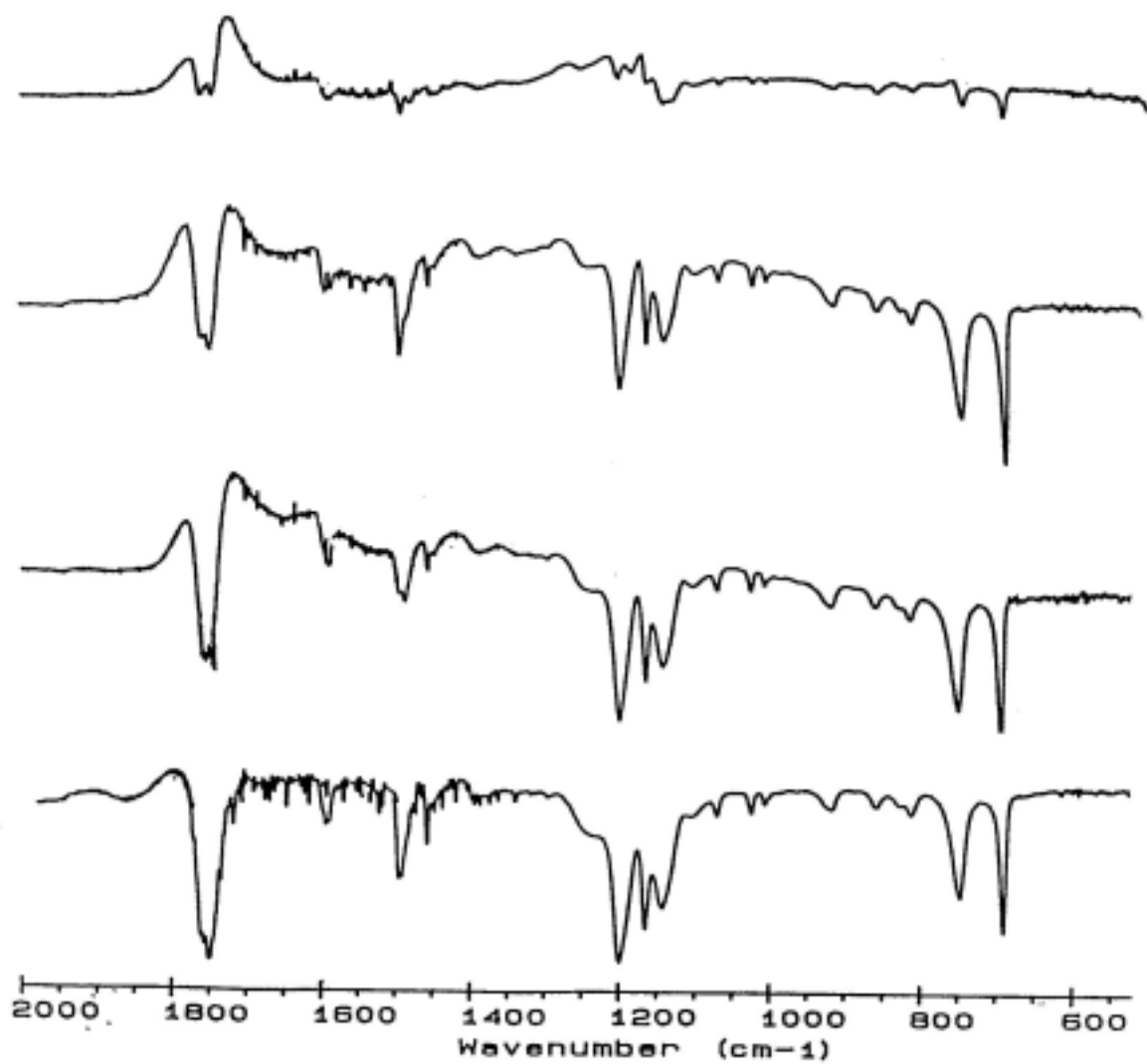


Figure 1-8 Typical difference spectra, $A_t - A_0$ (t in days), using benzene absorbance at 1595 cm^{-1} as internal standard.

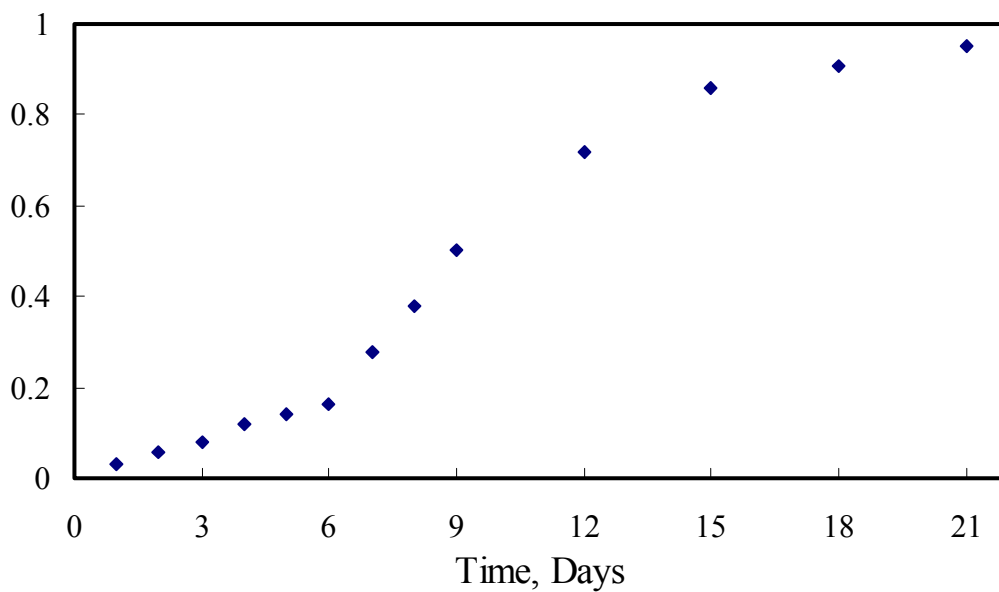


Figure 1-9 Plot of C-O-C disappearance conversion, α , versus irradiation time for PPA

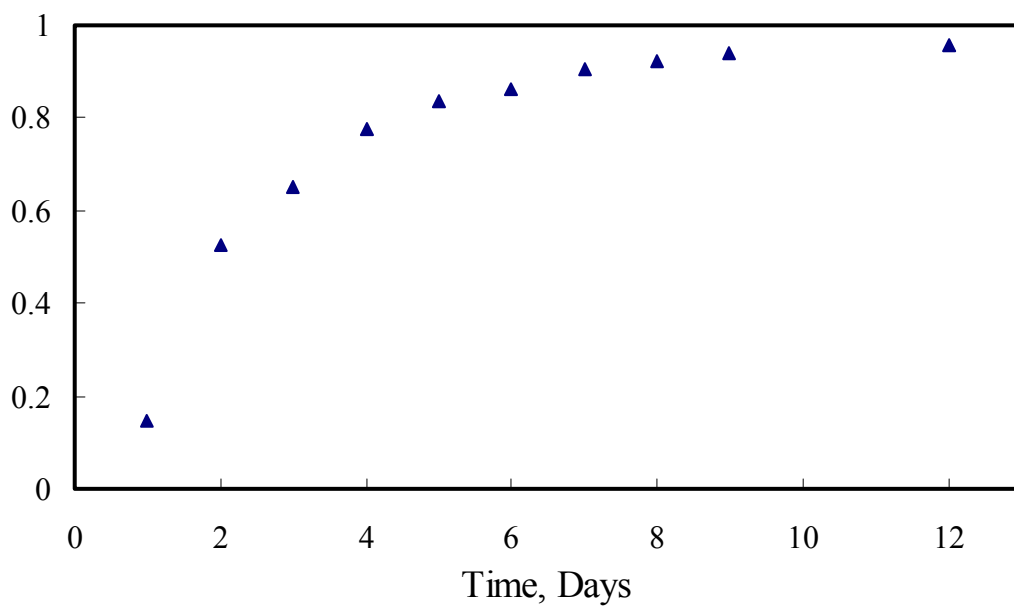


Figure 1-10 Plot of C-O-C disappearance conversion, α , versus irradiation time for PMPA

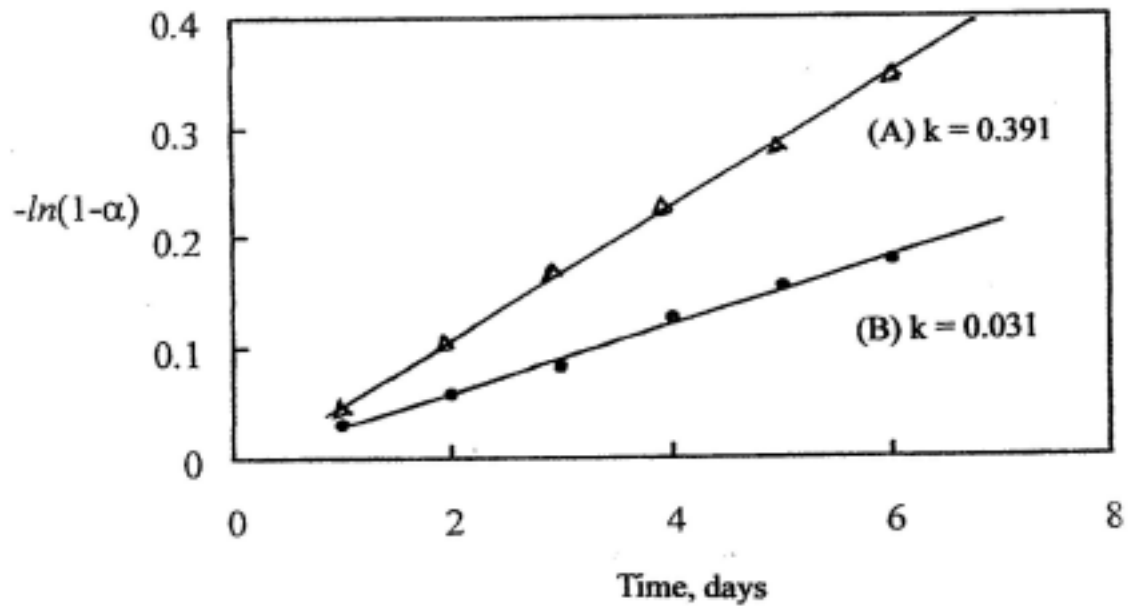


Figure 1-11 Plots of $-\ln(1-\alpha)$ versus time for (A) PMPA, and (B) PPA.

Chapter 2. Protection of PET Against Photodegradation by the Inherent Photo-stabilizers of Poly(phenyl acrylate) and Poly(p-methylphenyl acrylate)

2.1 ABSTRACT

Poly(phenyl acrylate) (PPA) and poly(p-methylphenyl acrylate) (PMPA) were used as inherent photo-stabilizers for PET in this study. PPA/PET and PMPA/PET in weight ratios of 0/100, 5/95, 10/90, 20/80 and 100/0 were blended. These blends were then cast into films and drawn into fibers and were irradiated with an accelerated weathering tester (QUV). Functional group changes in the films during irradiation were monitored with FTIR and the absorbance changes for different samples were compared with one another. Tensile strength of fibers after 42 days of irradiation were tested. Experimental results revealed that when incorporated with 5 % of PPA or PMPA into PET, good stabilization of the film and fibers were observed, with PMPA exhibiting more photo-stabilization capability and better retention of tensile strength after 42 days of accelerated ageing.

2.2 INTRODUCTION

PET is a commercially available polymer and is widely used as fiber, textile, bottle, video tape, food trays and other consumer products. Outdoor use of PET is very common. Therefore, its weatherability becomes an important consideration. Photo-stabilization of PET can be achieved by various means. These include screen of ultraviolet light, deactivation of excited states, addition of radical scavengers, and so on. Use of UV absorber to retard the adverse effect of irradiation is another possibility. The UV absorber absorbs harmful UV and converts it into a harmless form. However, discoloration may, sometimes, be a drawback. The most widely used UV absorbers are low molecular weight derivatives of o-hydroxybenzophenones, salicylic esters, and

benzotriazoles [1,2]. However, leaching might be a problem for these low molecular weight UV absorbers. Therefore, we are interested in using polymeric type of photo-stabilizers to avoid leaching problem and, in addition, to avoid the mechanical drawback. In our previous study on the kinetics of photo-fries rearrangement [3], both PPA and PMPA, upon irradiation of UV ranging from 275 to 360 nm, underwent intra-molecular photo-fries' rearrangement [4-9] with a first-order of reaction. We found that PPA produced both o- and p-hydroxybenzophenone moieties with a rate constant of $3.10 \times 10^{-2} \text{ day}^{-1}$, while PMPA produced only o-hydroxybenzophenone moiety with a rate constant of $3.91 \times 10^{-1} \text{ day}^{-1}$ [3]. Of the o- and p-hydroxybenzophenone, only the ortho form acts as an effective uv-absorber [1-3] since PMPA produced o-hydroxybenzophenone more effectively and therefore was believed to be a more effective inherent photo-stabilizer than PPA. In this paper, we report our further study on their field tests of photo-stabilization to PET.

2.3 EXPERIMENTAL

2.3.1 Sample Preparations

PPA and PMPA were synthesized as reported elsewhere [3]. PET with an intrinsic viscosity of 1.0 was obtained from Far Eastern Textile Ltd. (Taiwan). PPA/PET and PMPA/PET in weight ratios of 0/100, 5/95, 10/90, 20/80 and 100/0 were dissolved in phenol. Films were spin-coated on aluminum foil and dried in the vacuum oven overnight. The same weight ratios of PPA/PET and PMPA/PET were also blended with a brabender mixer, and then were drawn into fibers.

2.3.2 Instruments

Glass transition temperatures (T_g 's) were detected with Seiko SSC 5200 differential scanning calorimeter (DSC). Accelerated ageing tests were studied

with a Q-panel Company weathering tester with eight UVB-313 fluorescent UV lamps (each lamp 40 watts, wavelength ranging from 275 to 360 nm). Tensile strength of fibers were tested with an Orientec Tensilon RTA-1T with load cell of 1 Kg.

Functional group changes were investigated with a Nicolet 520 FTIR spectrometer with a resolution of 1 cm^{-1} . Difference spectra, $A_t - A_0$, were obtained by subtracting the absorbance at an irradiation time t from that before uv ageing, using the benzene absorbance at 1595 cm^{-1} as internal standard.

2.4 RESULTS AND DISCUSSION

PET undergoes photo-degradation and photo-oxidation when it is exposed in outdoor application. The degradation mechanisms and products are extensively reported in literature [10-12]. Degradation could result in deterioration of physical properties, such as loss of tensile strength and impact resistance, embrittlement, surface crazing and discoloration. Photodegradation degradation products include CO, CO₂, hydrogen, methane, ethane, benzyl end groups, etc.. By-products that are hydroxidized in the benzene ring and aliphatic position and few crosslinking molecules are also found. Figure 2-1 shows the ir spectrum of PET before degradation. Absorption at 3420 cm^{-1} is the overtone of $\nu_{\text{C=O}}$ at 1710 cm^{-1} for the ester group. $\nu_{\text{C-H}}$ of benzene ring occurs at 3050 to 3100 cm^{-1} . $\nu_{\text{C-H}}$ of saturated aliphatic hydrocarbons occurs at 2900 to 2980 cm^{-1} . The strong carbonyl absorption occurs at 1712 cm^{-1} . Benzene ring absorption occurs at 1500 to 1570 cm^{-1} . $\delta_{\text{H-C-H}}$ of the ethylene group occurs at 1460 to 1480 cm^{-1} . Absorption at 1420 cm^{-1} is due to $\delta_{\text{C-H}}$ of benzene ring bending in plane. Absorption at 1350 cm^{-1} is $\omega_{\text{C-H}}$ of wagging for ethylene glycol. Those at 1240 to 1280 cm^{-1} and at 1105 to 1130 cm^{-1} are due to $\nu_{\text{Ar-C(=O)-O}}$ and $\nu_{\text{C(=O)-O}}$, respectively. Absorption at 745 cm^{-1} is a typical frequency of the interaction between the polar ester and the benzene ring. Figure 2-2 shows the difference spectra of PET after various days of accelerated UV irradiation. It is noted that a continuous decrease of absorbances at 1712 ,

1270 to 1290 and 1135 to 1160 cm^{-1} are resultant of bond cleavage of ester group and ether linkage. The breakdown of 1,4-disubstituted bonds to the benzene ring was evidenced from the decreased absorbance at 745 cm^{-1} . These results agree well with reports in literature.

Figure 2-2 compares similar difference spectra of films for blends of PMPA/PET (10/90, 20/80), PMPA, PPA/PET (10/90, 20/80) and pure PET after 6 days of UV irradiation. The significant protection of scission at ester group can be evidenced from the retarded decreases of absorbances at 1712, 1270 to 1290 and 1135 to 1160 cm^{-1} . Our previous study on the kinetics of photo-fries' rearrangement for PMPA and PPA indicated that PMPA produced o-hydroxybenzophenone moiety linked to the side chain with a higher rate constant of $3.91 \times 10^{-1} \text{ day}^{-1}$, compared with a lower rate constant of $3.10 \times 10^{-2} \text{ day}^{-1}$ for PPA which produced both o- and p-hydroxybenzophenone moieties in the side chain (Figure 2-3). Of the two products, only o-hydroxybenzophenone contains a 6-membered ring structure with a labile H-bonding between OH and C=O and acts as a UV absorber [1,2]. This implied that PMPA would be a better inherent polymeric photo-stabilizer than PPA. Such a significant stabilization can be attributed to the good compatibility of PET/PMPA and PET/PPA. The miscibility of PMPA and PPA in PET in molecular level would provide good protection to PET. Figure 2-4 compares the Tg's for PET, PMPA and PET/PMPA blends. PET and PMPA have Tg's of 74.9 and 61.1 $^{\circ}\text{C}$, respectively. An inner shift of a single Tg at 66.0 $^{\circ}\text{C}$ for the PET/PMPA blend indicates a good compatibility of PET and PMPA. Similar finding was observed for the PET/PPA system (Figure 2-5). Figure 2-6 shows the percentage retention of tensile strength for fibers of PET, PET/PMPA (5/95, 10/90), and of PET/PPA (5/95, 10/90) blends after 7 days of accelerated uv irradiation. It is noted that PMPA played more significant photo-stabilization to PET than PPA under the same environment. This experimental result is well consistent with the functional group changes in FTIR monitoring (Figure 2-2) and our kinetic study for the photo-firies' rearrangement for PMPA and PPA

(Figure 2-3). Surprisingly enough fibers of the 10/90 of PMPA/PET and of PPA/PET indicate less retention of tensile strength, presumably because more low molecular weight portions of PMPA and PPA (with an average molecular weight of 9,700 and 9,600, respectively) in the blends drawback the mechanical property.

2.5 CONCLUSIONS

Both PPA and PMPA show good compatibility with PET and indicated significant stabilization of PET fiber against photo-oxidation in an accelerated weathering tester. PMPA indicated better photo-stabilization efficiency because PMPA, upon irradiation of UV, produced o-hydroxybenzophenone moiety linked to the side chain more efficiently. Tensile tests of fibers agreed well with functional group changes, as evidenced from FTIR difference spectra and the result of kinetic study. Higher level of low molecular weight PMPA or PPA incorporated into PET showed an adverse effect on the tensile strength of fibers.

2.6 REFERENCES

1. A. M. Trozzolo, "Stabilization Against oxidative photodegradation", in W. L. Hawkins edited, "Polymer Stabilization", Wiley-Interscience, New York, 1972, Ch.4, pp.198-202.
2. W. Schnable edited, "Polymer Degradation", Hanser International, distributed in USA by Macmillan Pub., New York, 1981, Ch.4, pp.118-120.
3. M. S. Lin, C. T. Lee and C. H. Wu, paper submitted to Polym. Degrad. & Stabil., 2003.
4. J. C. Anderson, and C. B. Reese, J. Chem. Soc., 1781 (1961).
5. J. C. Anderson, and C. B. Reese, Proc. Chem. Soc., 217 (1960).
6. S. K. L. Li, and J. E. Guillet, Macromolecules, 10(4), 840 (1977).
7. M. R. Sandner, E. Hefaya, and D. J. Trecker, JACS., 90, 7249 (1968).

8. H. Kobsa, *J. Org. Chem.*, 27, 2293 (1962).
9. R. A. Finnegan , and J. J. Mattice, *Tetrahedron*, 21, 1015 (1965)
10. R. Gachter and H. Muller, *Plastics additives Handbook*, 4th ed., (1993).
11. M. H. Tabankia and J. L. Gardette, *Polym. Degrad. & Stabil.*, 14, 351 (1986).
12. M. Day and D. M. Wiles, *J. Appl. Polym. Sci.*, 16, 203 (1972).

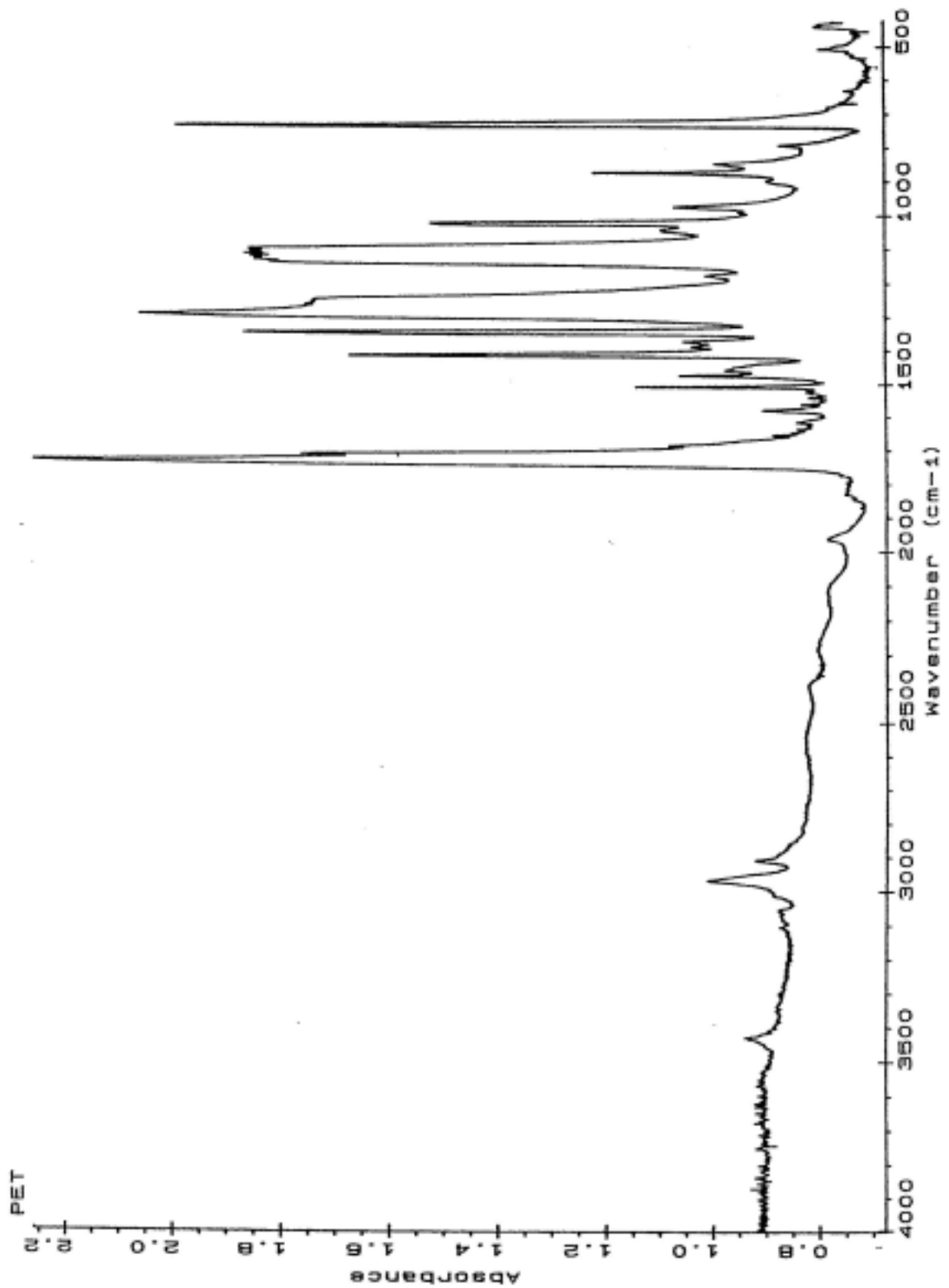


Figure 2-1 IR spectrum of PET before photodegradation.

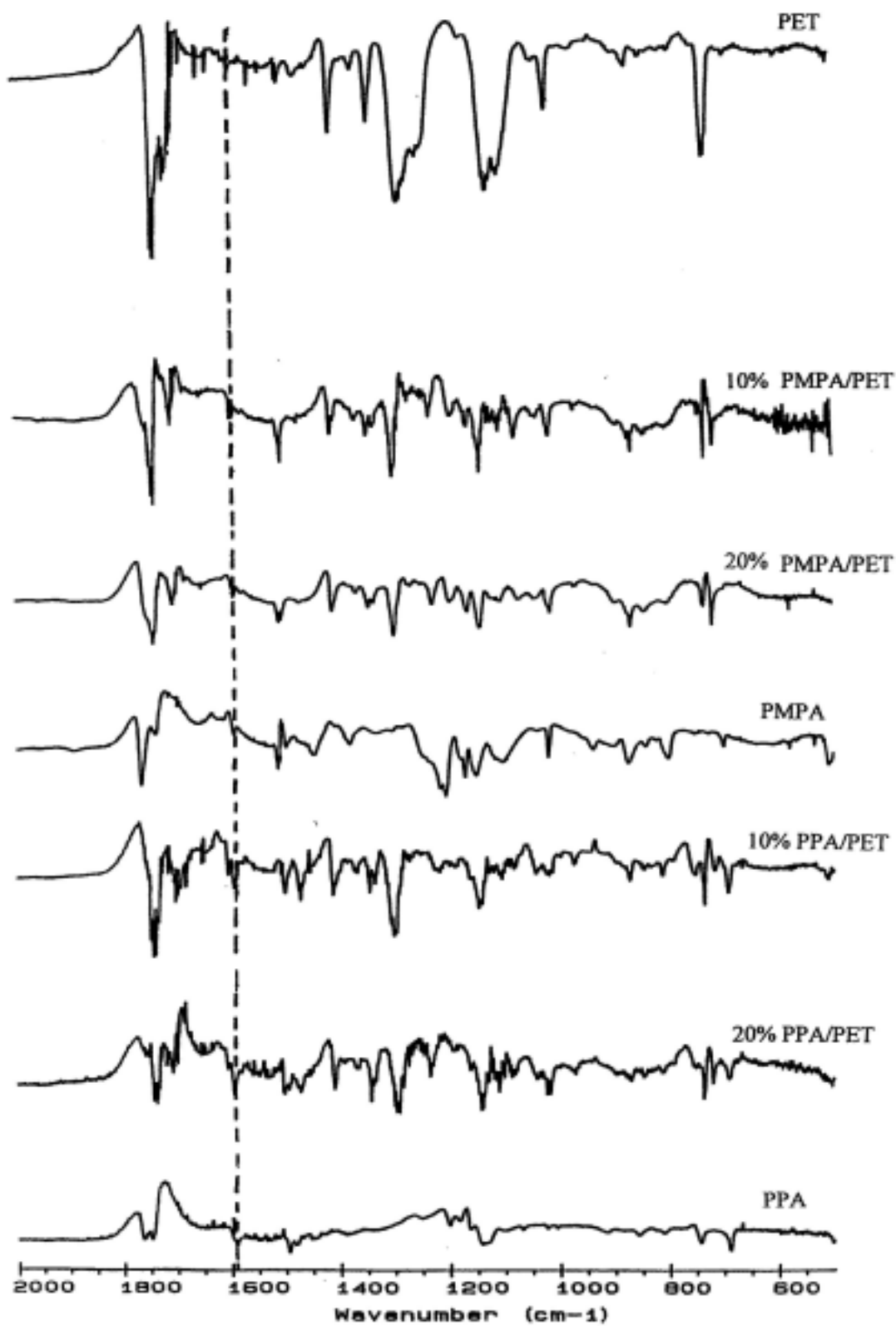


Figure 2-2 Typical difference spectra of samples (A_6 - A_0 , with benzene absorption as internal standard) after accelerated uv irradiation for 6 days.

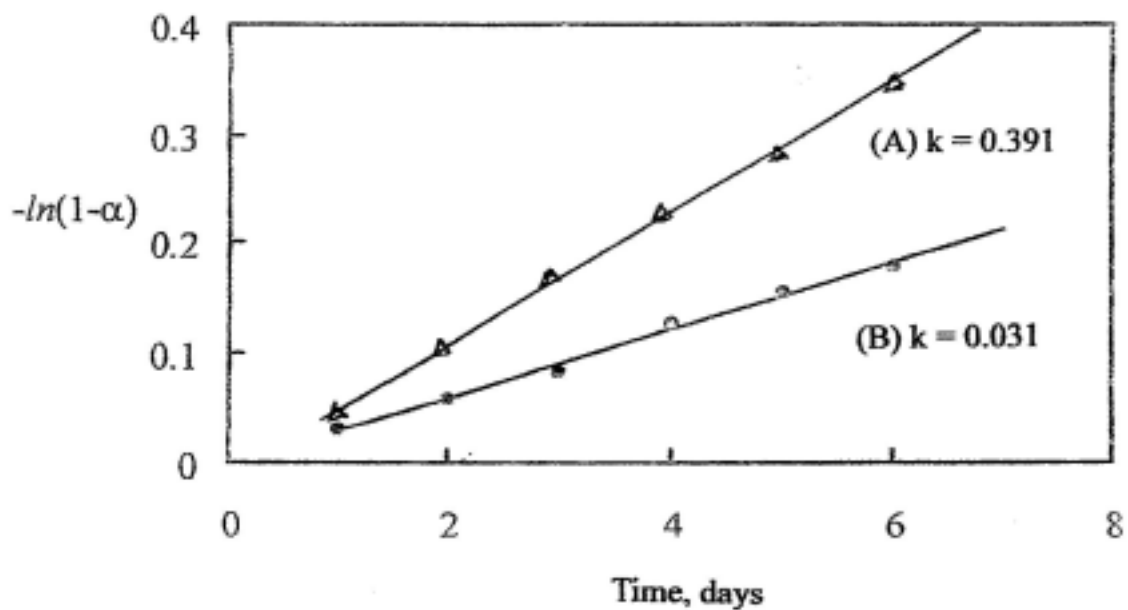


Figure 2-3 Plots of first-order rate expression, $-\ln(1-\alpha)$ vs. time, for photo-Fries' rearrangement of PMPA and PPA, where α is conversion. (A) PMPA with a rate constant, $k = 0.391$, and (B) PPA with $k = 0.0310$.

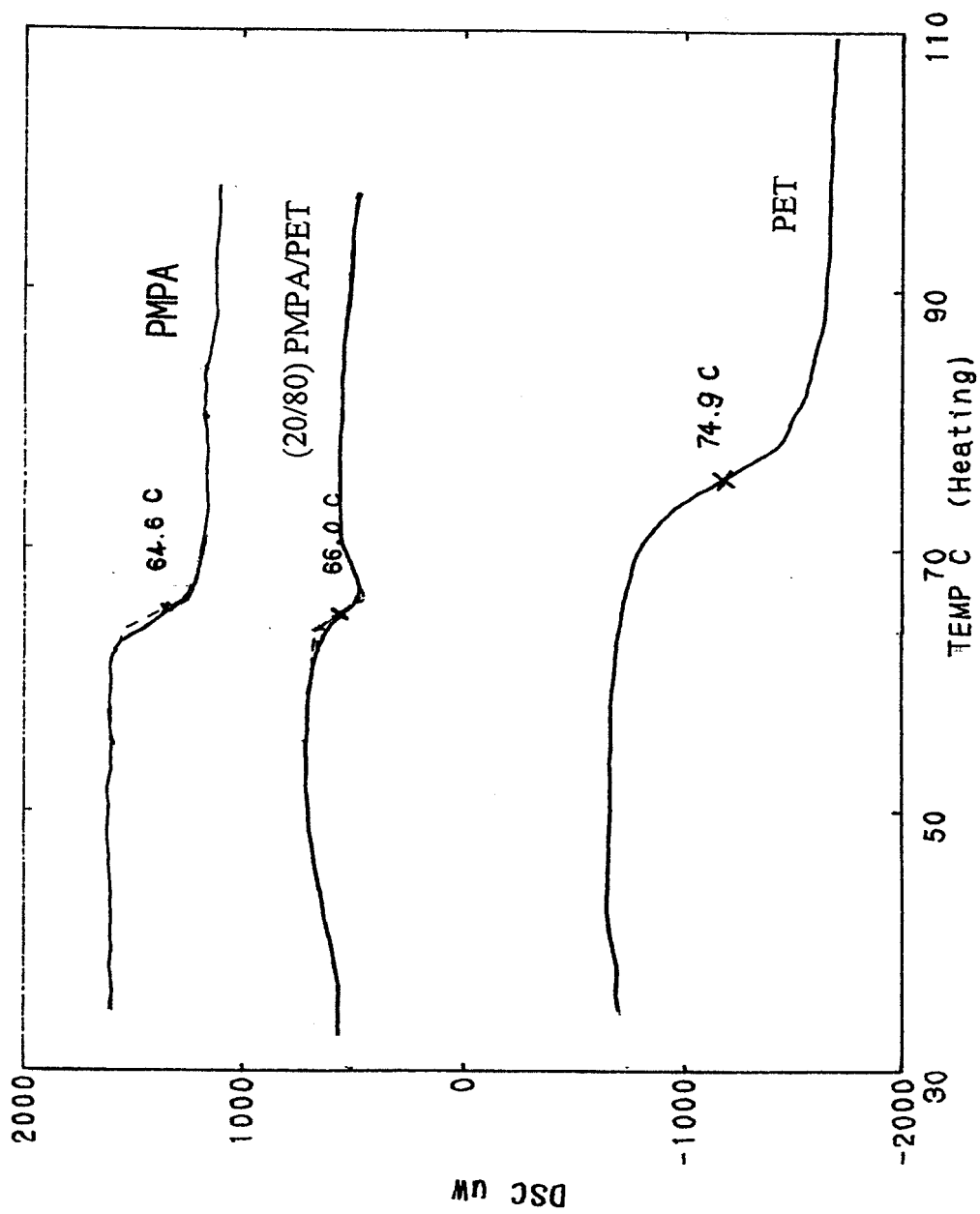


Figure 2-4 Comparisons of Tg's for PET, PMPA and PET/PMPA blends.

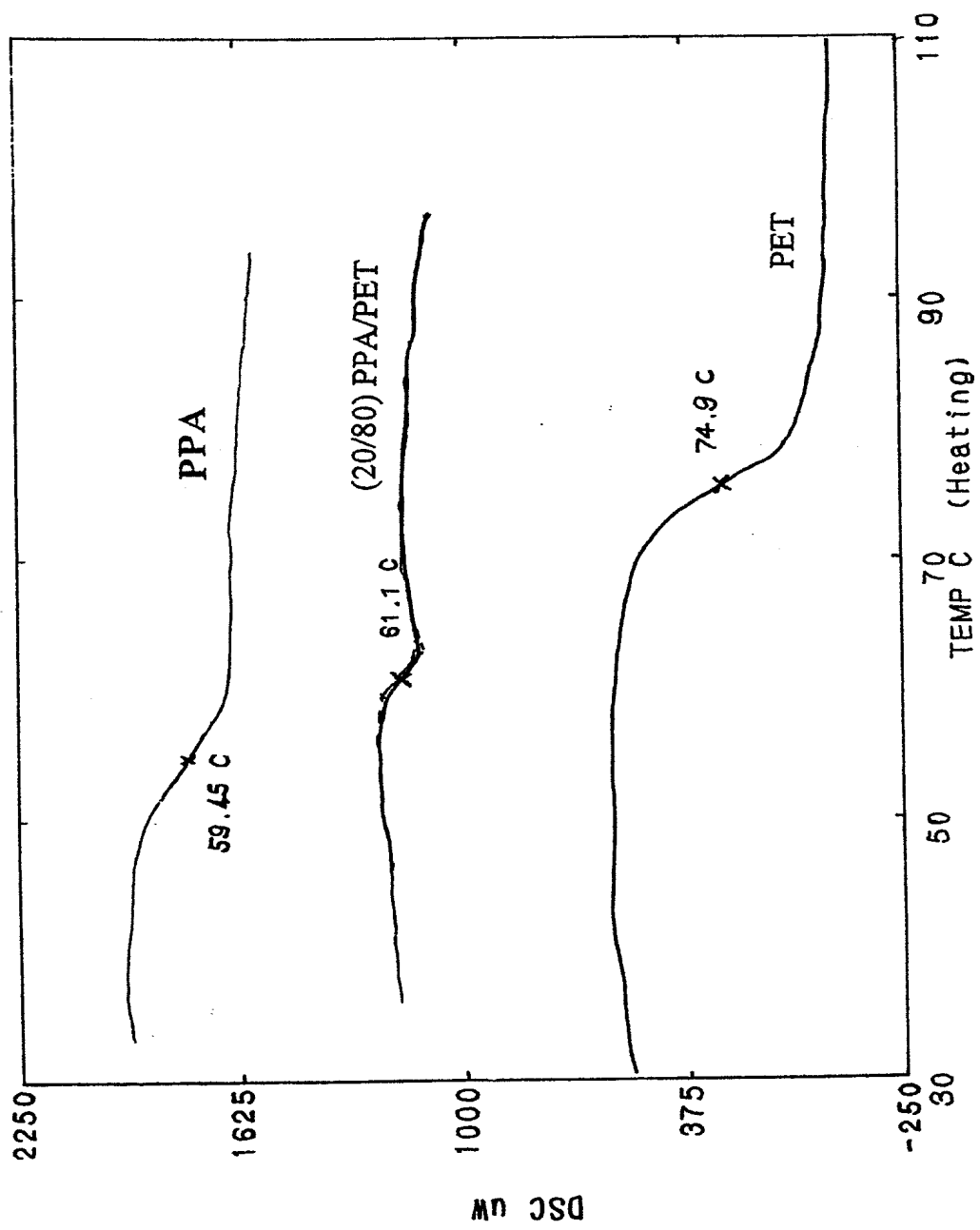


Figure 2-5 Comparisons of Tg's for PET, PPA and PET/PPA blends.

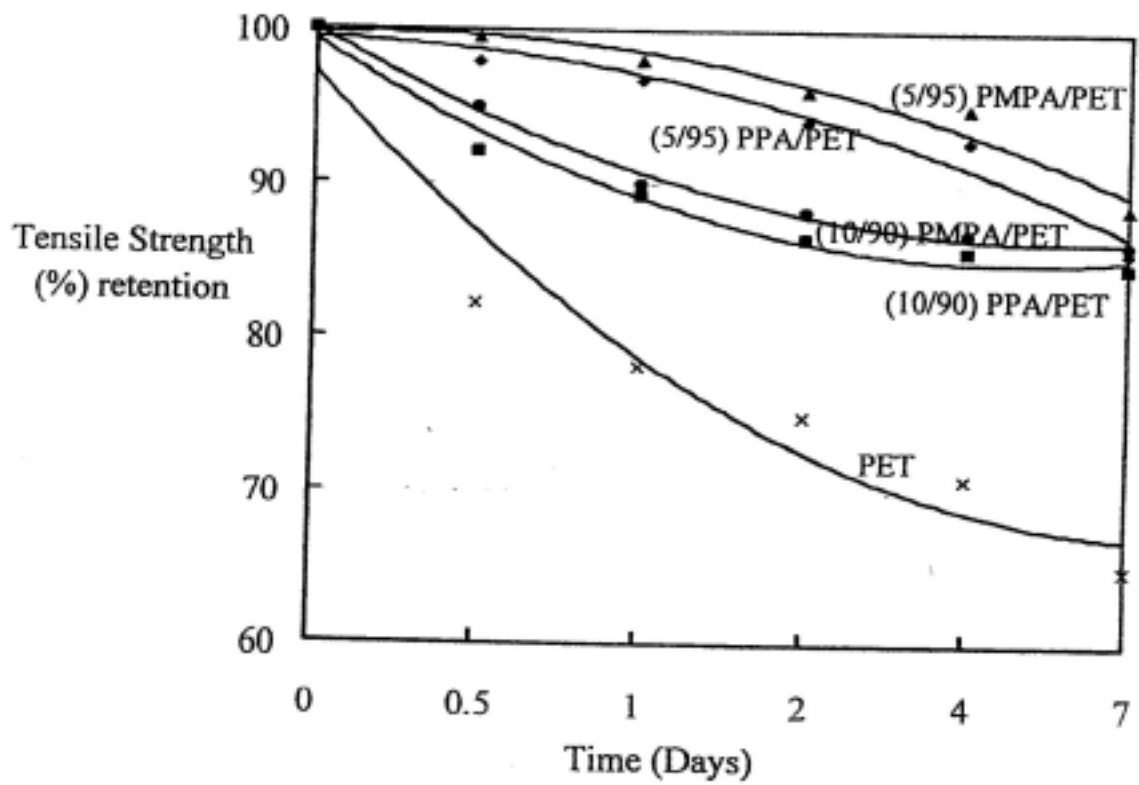


Figure 2-6 Percentage retention of tensile strength for fibers of PET, PET/PMMA (5/95, 10/90) and PET/PPA (5/95, 10/90) blends after 7 days of accelerated ageing.

Chapter 3 Photostabilization of an Epoxy Resin by Forming IPNs with Bisphenol-A Diacrylate

3.1 ABSTRACT

Bisphenol-A diacrylate (BADA) was synthesized from the reaction of bisphenol-A and acryloyl chloride. Interpenetrating polymer networks (IPNs) based on diglycidyl ether of bisphenol-A (DGEBA) and BADA in weight ratios of DGEBA/BADA = 100/0, 75/25, 50/50 and 25/75 were prepared by using 4,4'-diaminodiphenylmethane (MDA) and benzoyl peroxide (BPO) as curing agents. Samples were irradiated with ultraviolet in a Q-UVA weather-o-meter to study their ageing behavior. Experimental results indicated that the BADA thus incorporated in the IPN structure confers significant photostabilization of the epoxy, as shown by less chain scission at C-O-C in the epoxy, with less property loss in mechanical tests.

3.2 INTRODUCTION

Epoxy resins exhibit excellent physical properties and good adhesion, and are widely used in such areas as coatings, adhesives, composites, encapsulants, etc. Photodegradation of epoxies is important and was reported by DICKENS ET AL. [1] and also by others [2-6]. A survey of the photo-oxidation of DGEBA indicates damage of the epoxy resin, resulting in chain scission, leading to deterioration of physical properties. It is well known in literature that phenyl benzoates, upon irradiation with ultraviolet, undergo Photo-Fries' rearrangement, leading to the formation of o-hydroxyphenyl ketone which contains a hydrogen bonded six-membered ring structure and acts as a UV absorber [7-10]. Incorporation of such a moiety into an epoxy may significantly stabilize the epoxy resin against photodegradation. In view of the structure of bisphenol-A diacrylate, the Photo-Fries' rearrangement would lead to a structure similar to a UV absorber. It is highly that an IPN

containing such a moiety would act as a photostabilizer. In this article we report such results in our studies.

3.3 EXPERIMENTAL

3.3.1 Preparation of bisphenol-A diacrylate (BADA)

Into a 3-l three necked flask, equipped with a mechanical stirrer and a thermometer, 1 mol of bisphenol-A was charged. Enough methyl ethyl ketone (MEK) was added to dissolve the bisphenol-A. Two mol of NaOH (80g) and 2 mol of triethylamine were added. The mixture was kept below 5 °C. Then 2 mol of acryloyl chloride was added dropwise keeping the temperature near 5 °C. The acrylation continued for 10 h. The reaction mixture was poured into a large quantity of deionized water. A crude yellow product was obtained with a yield of 96%. A white crystal with m.p. 95-96 °C was obtained after recrystallization from *n*-hexane/ CH₂Cl₂(v/v 4/1).

3.3.2 Preparation of DGEBA/BADA IPNs

Blends of DGEBA/BADA in weight ratios of 100/0, 75/25, 50/50 and 25/75 were prepared. BPO (1 phr based on BADA) and MDA (in stoichiometric equivalence of DGEBA) were added as curing agents. To prepare specimens, each composition was mixed and deformed thoroughly and poured into Teflon moulds, then pre-cured at 80 °C for 4 h, followed by curing at 140 °C for another 4 h, and finally post-cured at 180 °C for 2 h.

3.3.3 Instruments

Functional group changes during ageing were monitored with a Fourier transform infrared spectrometer (FTIR, Nicolet 520 with a resolution of 0.5 cm⁻¹). Thin films were spin coated on Aluminum plates and cured, then irradiated in a QUV-A weather-o-meter for various times. The difference spectra were obtained by subtracting the spectrum at time *t* from that before

ageing, using benzene absorption 1609 cm^{-1} as internal standard. Test specimens were prepared according to the method mentioned and were also subject to irradiation in the QUV-A weather-o-meter. Impact resistance was examined with a falling dart type impact tester, with a dart weight of 3.3kg. The energy under the curve was integrated automatically. Tensile and elongation tests were performed according to an ASTM D638 type 1. The test speed was set at 5 mm min^{-1} . An average of 5 test values reported for all mechanical properties.

3.4 RESULTS and DISCUSSION

The synthesized BADA has the following chemical structure

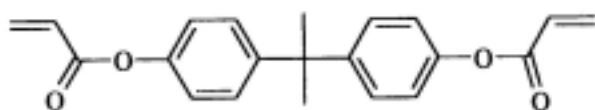
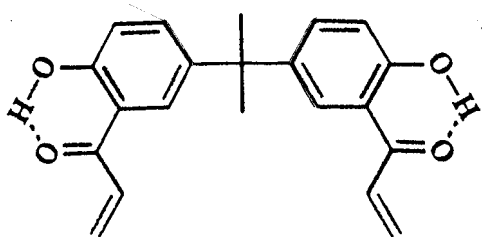


Figure 3-1 shows its ^1H NMR spectrum in CDCl_3 . The 6 H's of the two methyl groups occur at 1.63 ppm . The 8 H's of the two phenyl rings (He) occur at 7.01 and 7.26 ppm (quartet). The 4 H's at the two terminal vinyl hydrogens occur at 5.98 ppm (cisH_b, doublet), while the other 2 H's at the two vinyl groups (Hc) occur at 6.35 ppm (quartet). Figure 3-2 shows its FTIR Spectrum. The strong carbonyl absorption of the ester group at 1733 cm^{-1} and the moderate absorption of C=C at 1623 cm^{-1} confirm the structure. Free radical polymerization of BADA by BPO resulted in a network structure via a chain mechanism, while curing of DGEBA with MDA resulted in another network structure via step mechanism [11]. Simultaneous curing of various blends of BADA(BPO)/DGE-BA(MDA) would lead to various compositions of IPNs via two independent reaction mechanisms. The two components, BADA and DGEBA, have good compatibility,

as evidenced by a single glass transition in dsc thermograms (Figure 3-3) and a single damping peak from the rheometric dynamic spectroscopy (RDS, Figure 3-4) for each IPN [12].

Upon long term irradiation with ultraviolet, the BADA moiety underwent Photo-Fries' rearrangement and led to a six-membered ring structure with an intramolecular H-bonding [10].



This reaction is well known in literature [10,13]. The o-hydroxybenzophenone thus produced indicated a strong intramolecular hydrogen-bonding between the hydroxyl and carbonyl groups. This intramolecular hydrogen-bonded six-membered ring structure dissipated the UV energy through a physical process [10]. The miscibility of BADA and DGEBA in the IPNs provided good photo protection of the material. Figure 3-5 shows the difference spectra of FTIR for the cured DGEBA, BADA, and 50/50 IPN. The difference spectra $A_t - A_0$ means the spectra obtained by subtracting the absorbance at t (in days) from that before irradiation. It is obvious from Figure 3-5 that the decreasing absorbance at 1265 cm^{-1} indicated the bond breaking of the C-O-C bond in the main chain of cured DGEBA [13]. This type of bond breaking has been well known in literature [1-9]. Continued decrease of absorbance at 1265 cm^{-1} with time is clear from Figure 3-5. Similar phenomenon, but less decrease at 1265 cm^{-1} in the 50/50 IPN is observed from Figure 3-6, indicating less chain scission at C-O-C bond in the IPN. This result strongly supports a significant photostabilization of DGEBA by BADA.

Figures 3-7 and 3-8 show the % retention of stress and of strain for DGEBA/BADA IPNs of 100/0, 75/25, 50/50 and 25/75 after 45 days of

irradiation. [Figure 3-9](#) shows the corresponding % retention of impact resistance. All these mechanical property retention strongly support the photostabilization of the epoxy by forming IPN with BADA.

3.5 CONCLUSIONS

Long term accelerated UV ageing of DGEBA resulted in a main chain scission at C-O-C bonds as evidenced from the decreased absorbance at 1265 cm^{-1} in FTIR spectra. Photostabilization of the epoxy resin by forming IPN with bisphenol-A diacrylate can be achieved. This protection resulted in mechanical property retention of the DGEBA/BADA IPN materials.

3.6 REFERENCES

1. Dickens B, Martin JW, Waksen D. *Polymer* 1984;25:706.
2. Zhang G, Pitt WG, Goates SR, Owen NL. *J Appl Polym Sci* 1994;54:419.
3. Rivaton A, Moreau L. *Polym Degrad Stab* 1997;58:321.
4. Rivaton A, Moreau L. *Polym Degrad Stab* 1997;58:333.
5. Grassie N, Guy MI. *Polym Degrad Stab* 1985;13:249.
6. Grassie N, Guy MI. *Polym Degrad Stab* 1986;16:53.
7. Sander MR, Hedaga E, Trecken DJ. *J Am Chem Soc* 1968;90:7249.
8. Meyer JM, Hammond GS. *J Am Chem Soc* 1972;94:2219.
9. Copping GM, Bell ER. *J Phys Chem* 1966;70:3479.
10. Schnabel W, editor. *Polymer degradation*. New York: Hanser International, Macmillan Publishing Co, 1981. P.118.
11. Odian G, editor. *Principles of polymerization*. 3rd. ed. New York: John Wiley & Sons, 1990 (Chapters 2 and 3).
12. Lin MS, Yeh CC. *J Polym Sci* 1993;31:2093.
13. Lin MS, Wang MW, Lee CT, Shao SY. *Polym Degrad Stab* 1998;60:505.

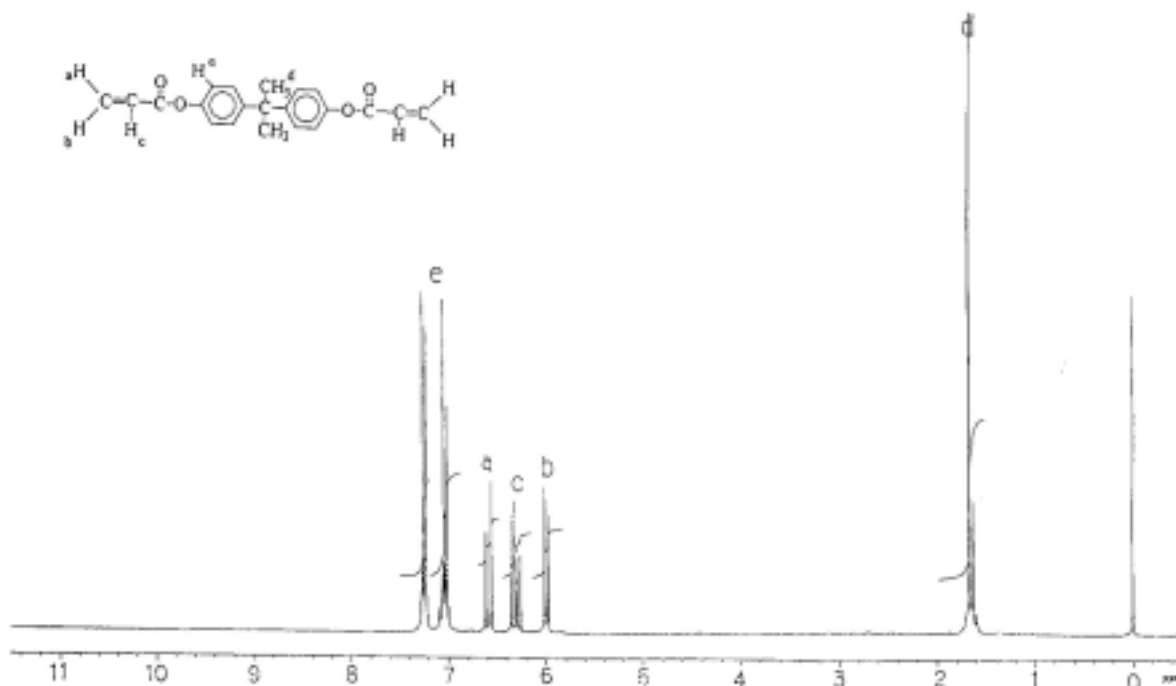


Figure 3-1 ^1H NMR spectrum of BADA in CDCl_3 .

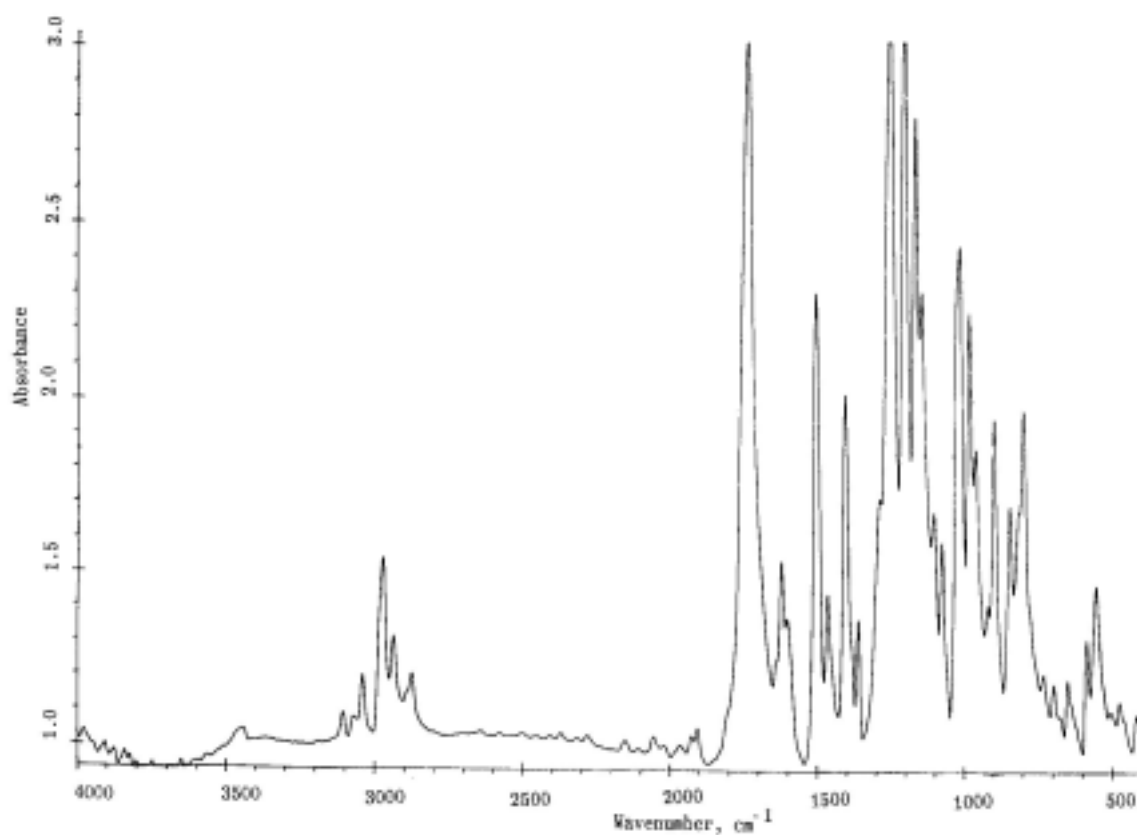


Figure 3-2 FTIR spectrum of BADA.

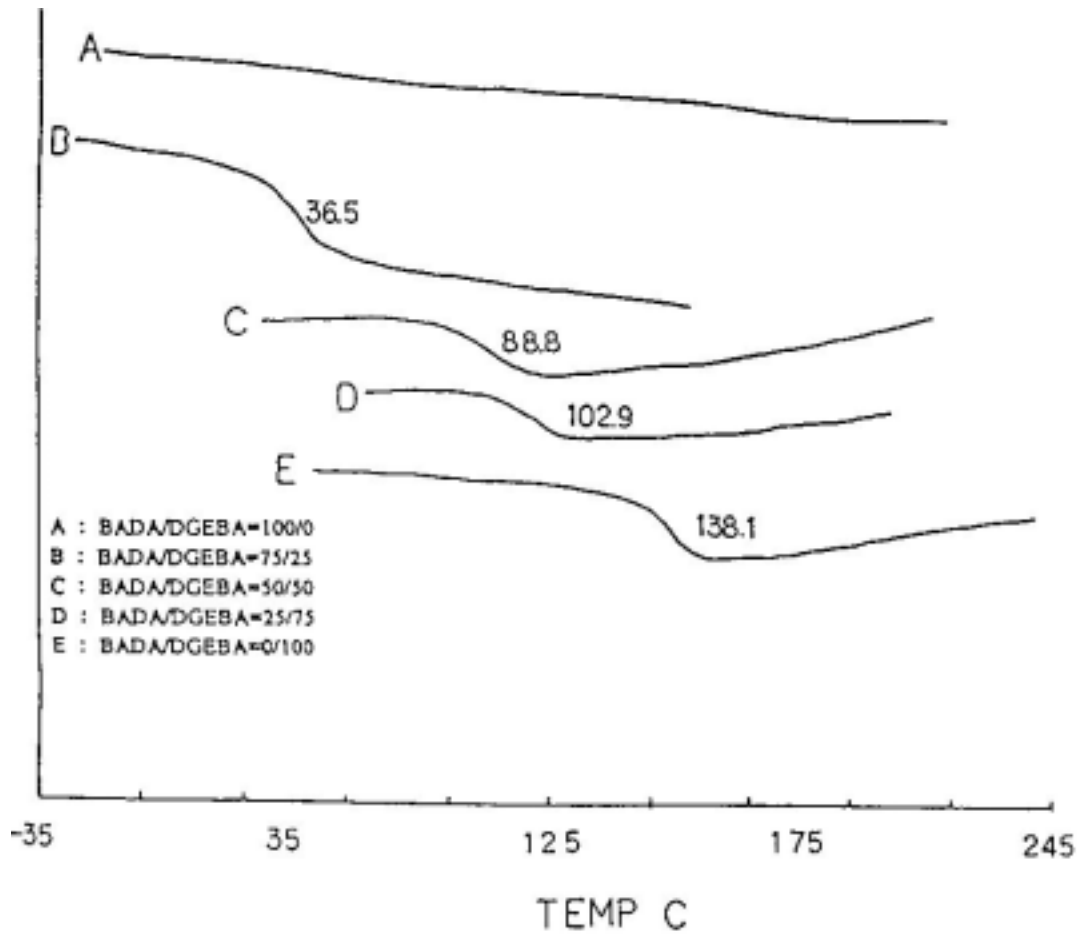


Figure 3-3 DSC thermograms for various BADA/DGEBA IPNs.

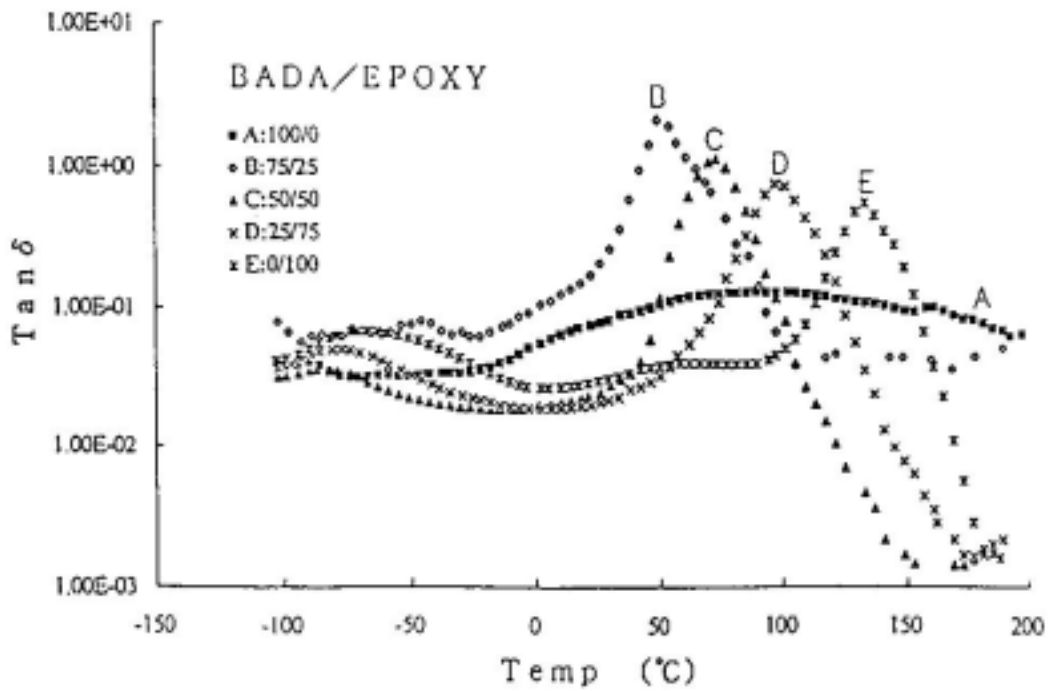


Figure 3-4 RDS curves showing the shifts of damping peaks for various BADA/DGEBA IPNs.

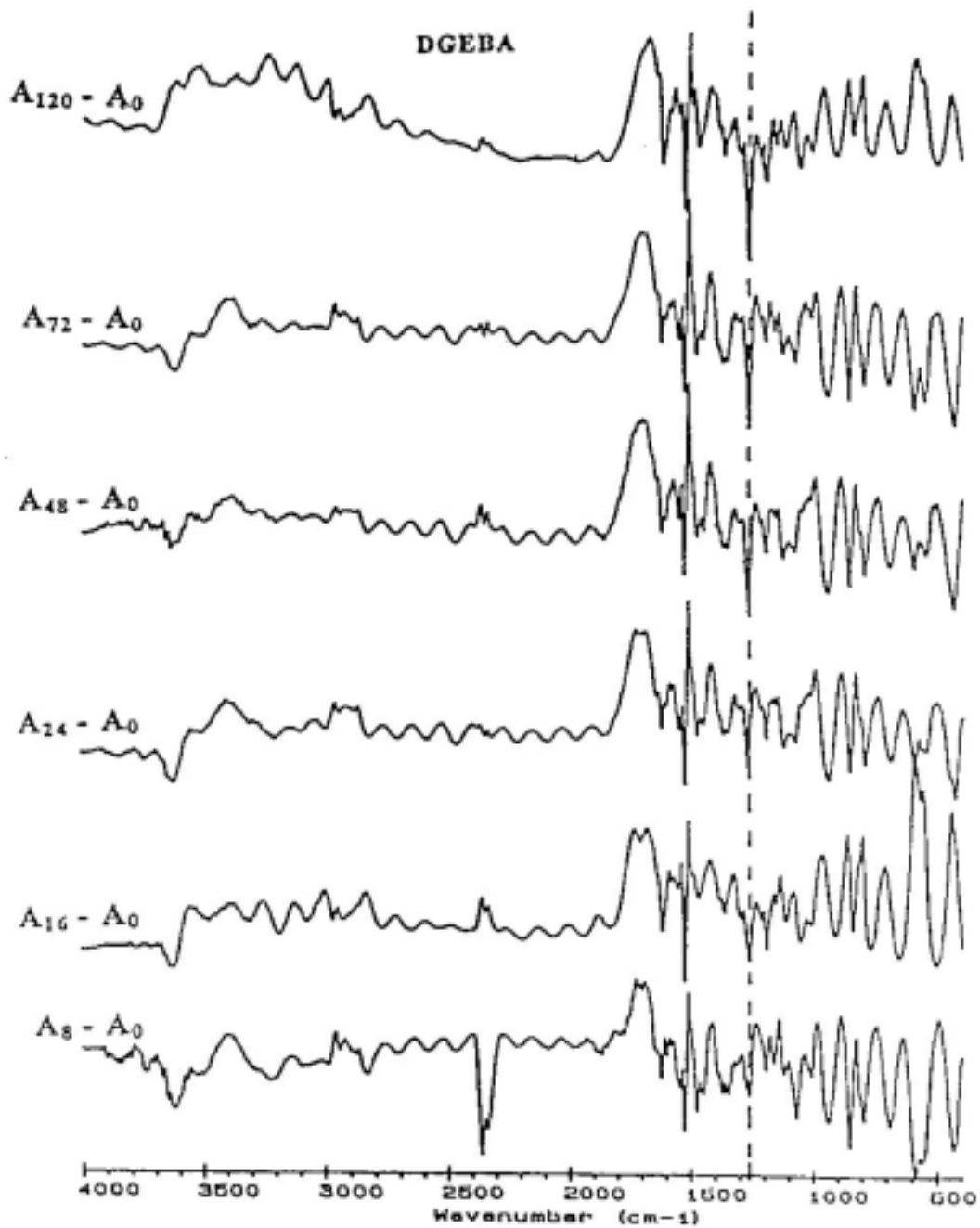


Figure 3-5 Difference spectra ($A_t - A_0$, t in days) for pure DGEBA.

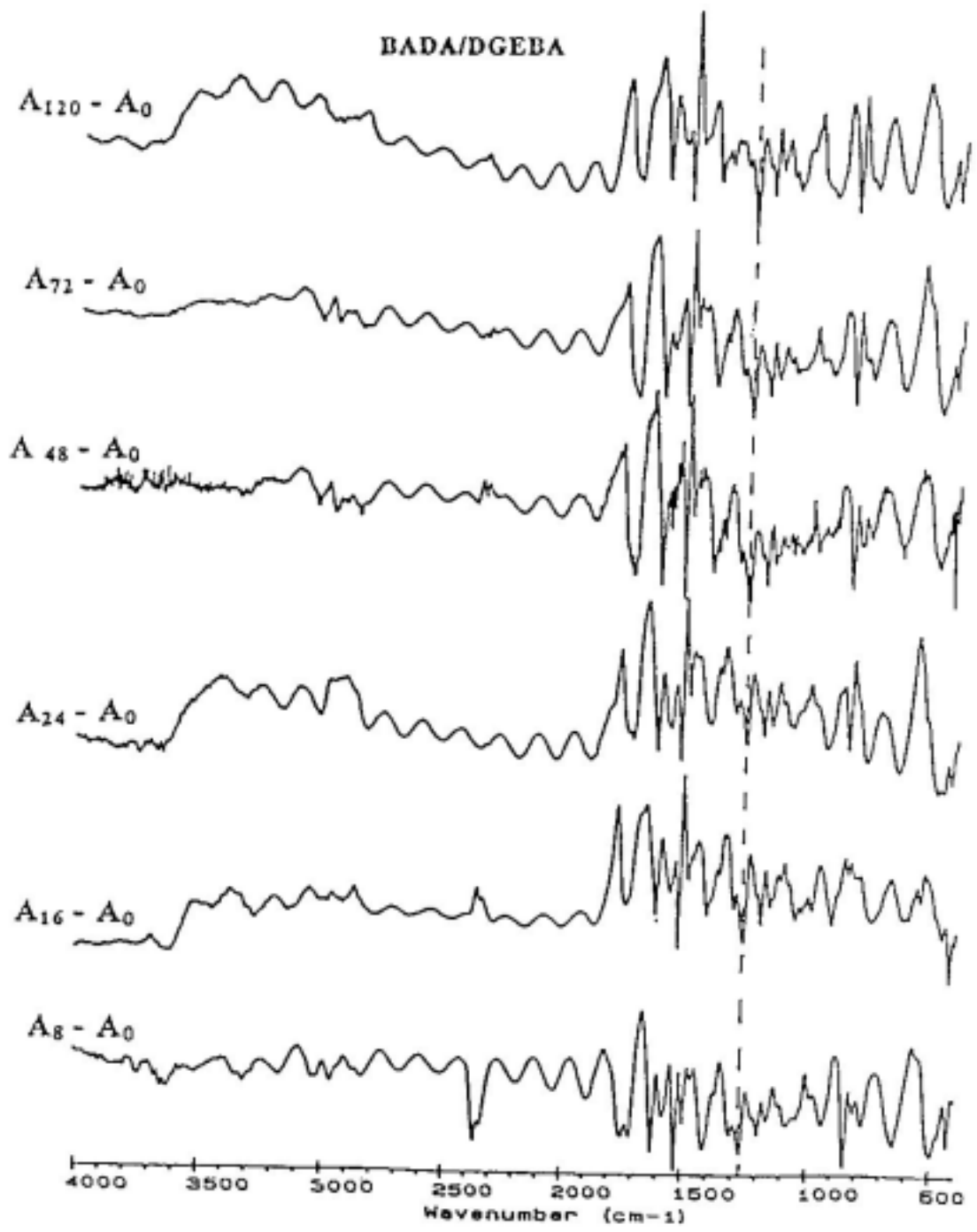


Figure 3-6 Difference spectra ($A_t - A_0$, t in days) for 50/50 of BADA/DGEBA IPN.

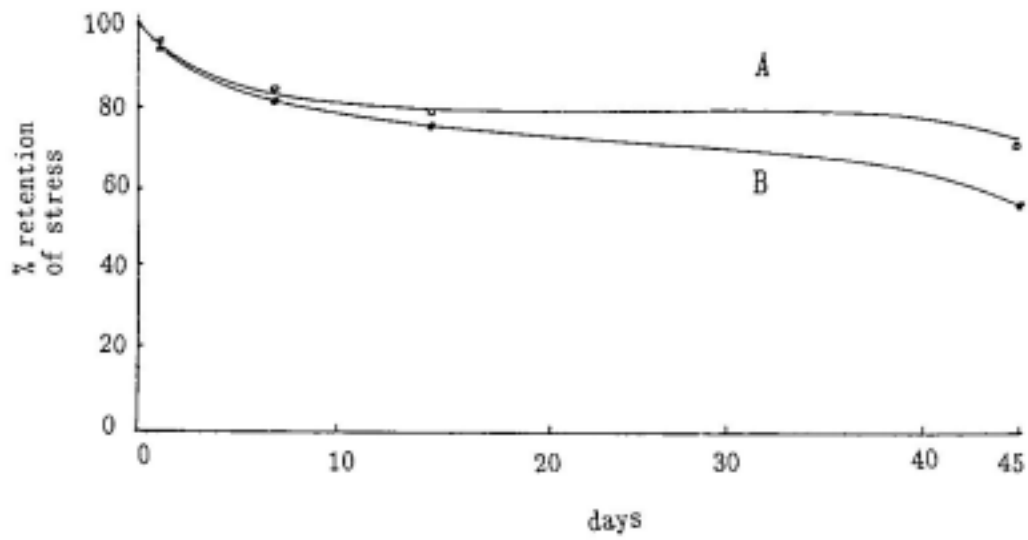


Figure 3-7 Plots of % retention of stress at break versus irradiation time. A: IPN, B:DGEBA.

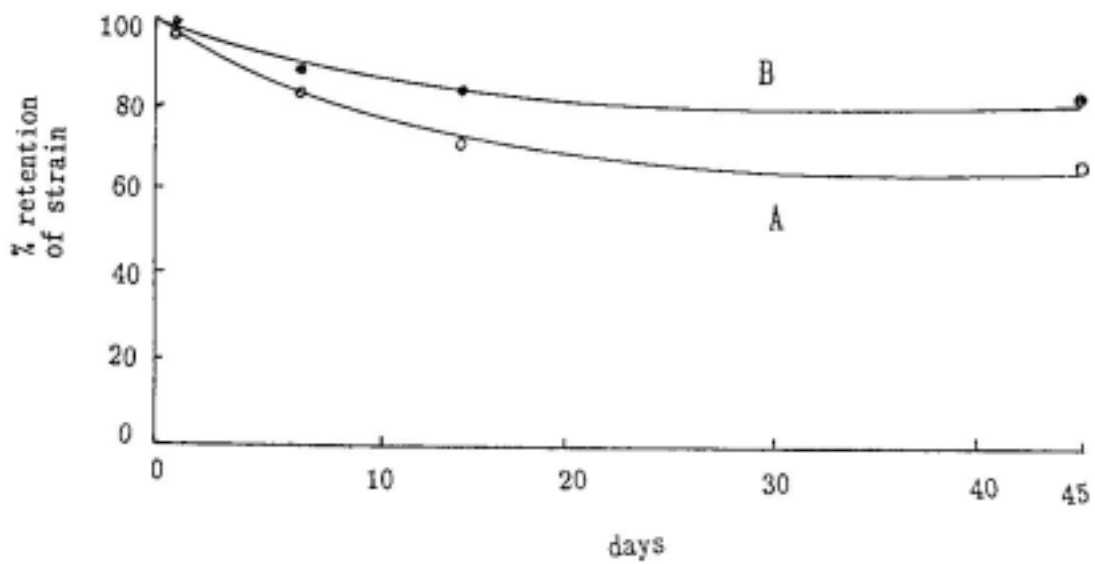


Figure 3-8 Plots of % retention of strain at break versus irradiation time. A: IPN, B:DGEBA.

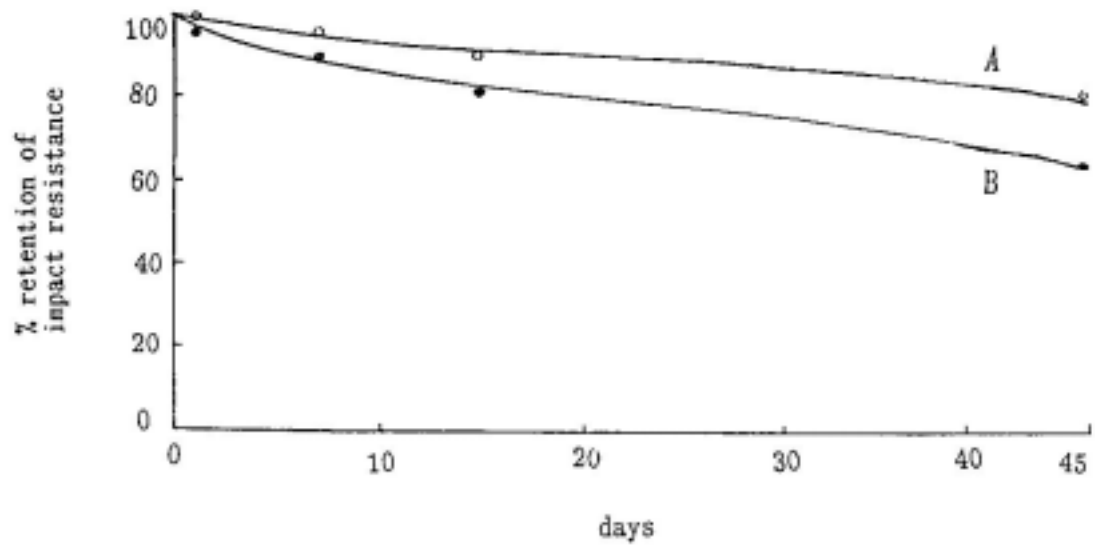


Figure 3-9 Plots of % retention of impact resistance versus irradiation time. A: IPN, B:DGEBA.